Fohlmeister, J., Plessen, B., Dudashvili, A. S., Tjallingii, R., Wolff, C., Gafurov, A., Cheng, H. (2017): Winter precipitation changes during the Medieval Climate Anomaly and the Little Ice Age in arid Central Asia. - *Quaternary Science Reviews*, *178*, pp. 24—36.

DOI: http://doi.org/10.1016/j.quascirev.2017.10.026

Winter precipitation changes during the Medieval Climate Anomaly and the Little Ice Age in arid Central Asia

Jens Fohlmeister [1,*], Birgit Plessen [2], Alexey Sergeevich Dudashvili [3], Rik Tjallingii [2], Christian Wolff [1,4], Abror Gafurov [5], Hai Cheng [6,7]

1 Institute of Earth and Environmental Science, University of Potsdam, Karl-Liebknecht-Strasse 24, D-14476, Germany

2 Helmholtz Centre Potsdam, GFZ German Research Centre for Geosciences, Section 5.2 Climate Dynamics and Landscape Development, Telegrafenberg, D-14473 Potsdam, Germany

3 Fund of Preservation and Exploration of Caves (Kyrgyzstan)

4 Max Planck Institute for Chemistry, Climate Geochemistry Department, D-55128 Mainz, Germany

5 Helmholtz Centre Potsdam, GFZ German Research Centre for Geosciences, Section 5. 4 Hydrology, Telegrafenberg, D-14473 Potsdam, Germany

6 Institute of Global Environmental Change, Xi'an Jiaotong University, Xi'an, Shaanxi, 710049, China

7 Department of Geology and Geophysics, University of Minnesota, Minneapolis, MN 55455, USA

* corresponding author; contact details: email: jens.fohlmeister@uni-potsdam.de,

Tel: 0049 (0)331 9775435

Abstract

The strength of the North Atlantic Oscillation (NAO) is considered to be the main driver of climate changes over the European and western Asian continents throughout the last millennium. For example, the predominantly warm Medieval Climate Anomaly (MCA) and the following cold period of the Little Ice Age (LIA) over Europe have been associated with long-lasting phases with a positive and negative NAO index. Its climatic imprint is especially pronounced in European winter seasons.

However, little is known about the influence of NAO with respect to its eastern extent over the Eurasian continent.

Here we present speleothem records ($\delta^{13}C$, $\delta^{18}O$ and Sr/Ca) from the southern rim of Fergana Basin (Central Asia) revealing annually resolved past climate variations during the last millennium. The age control of the stalagmite relies on radiocarbon dating as large amounts of detrital material inhibit accurate ^{230}Th dating. Present-day calcification of the stalagmite is most effective during spring when the cave atmosphere and elevated water supply by snow melting and high amount of spring precipitation provide optimal conditions. Seasonal precipitation variations cause changes of the stable isotope and Sr/Ca compositions. The simultaneous changes in these geochemical proxies, however, give also evidence for fractionation processes in the cave. By disentangling both processes, we demonstrate that the amount of winter precipitation during the MCA was generally higher than during the LIA, which is in line with climatic changes linked to the NAO index but opposite to the higher mountain records of Central Asia. Several events of strongly reduced winter precipitation are observed during the LIA in Central Asia. These dry winter events can be related to phases of a strong negative NAO index and all results reveal that winter precipitation over the central Eurasian continent is tightly linked to atmospheric NAO modes by the westerly wind systems.

1. Introduction

Annually resolved regional climate records play a vital role in understanding the nature of rapid climate changes and validation of present and future climate modelling (Mayewski et al. 2004.) The last millennium is characterised by climatic extremes of the generally warm Medieval Climate Anomaly (MCA), the cold Little Ice Age (LIA) and the subsequent present-day warm period since the beginning of the 19th century (for reviews, e.g., Bradley et al., 2003; Jones et al., 2009; Trouet et al., 2012). However, these climatic variations lack a clear global fingerprint and are only apparent from regional and seasonal expressions (Bradley et al., 2003; Graham et al., 2011).

European climate records reveal that the MCA, and LIA are associated with the strength and phases of the North Atlantic Oscillation (NAO; e.g., Hurrell et al., 1995; Wanner et al., 2001; Trouet et al., 2009). The NAO index is defined in terms of differences in anomalies of sea level pressure fields between the Azores and Iceland (e.g., Van Loon and Rogers, 1978; Meehl and Van Loon, 1979; Lamb and Peppler, 1987). It appears that NAO is most important for winter climate (Wanner et al., 2001; Trouet et al., 2009) but a large number of studies show that also the summer NAO can influence the climate on the European continent (e.g., Folland et al., 2009; Linderholm et al., 2013; Favá et al., 2016). A positive winter NAO index is related to strong westerly winds north of the European Alps influencing the climate most likely towards deep into the northern Eurasian continent. Those conditions are often related to relatively warm and wet winters in northern Europe. In contrast, colder and drier winters are expected during predominantly negative winter NAO index conditions. An opposite pattern is expected for southern Europe and the Mediterranean.

An unsolved question is about the eastwards influence of the NAO within the last millennium. Correlation analysis of present day winter precipitation in Central Asia with the strength of NAO suggests a negative relationship (Aizen et al., 2001). The influence of NAO on Central Asia during the past was not shown yet, since high resolution records from Central Asia are only sparse. A few well dated tree-ring data covering approximately the last 1000 years from the area around the eastern Tian Shan exist (e.g., Esper et al., 2002; 2003). Those records, however, are archives, which preferably record summer conditions and are less suited to prove the influence of winter NAO conditions on climate in this region. Furthermore, lake-sediment data (Taft et al., 2014; Lauterbach et al., 2014; Huang et al., 2011; Sorrel et al., 2007) are available, which recorded winter conditions, but unfortunately lacks a high resolution signal and partly suffer from dating uncertainties during the period of the last millennium. Nevertheless, findings from Lauterbach et al. (2014) and Huang et al. (2011) are in contrast to the analysis by Aizen et al. (2001) as they show a positive relationship between winter precipitation and NAO during the late Holocene. Recently, a precisely dated stalagmite from the western Tian Shan realm showed excursions in its stable oxygen isotope signal, which is interpreted to respond on precipitation changes (i.e., on the amount of rain provided by winter Westerlies), but did not record large parts of the last millennium (Wolff et al., 2017).

Speleothems from the mid-latitudes of the Northern hemisphere often proved to provide information about climate variability for the winter season (e.g., Niggemann et al., 2003, Wackerbarth et al., 2010; Fohlmeister et al., 2012; 2013; Scholz et al., 2012). In this paper, the examination of a speleothem from the western Tian Shan realm reveals also its capacity to record winter climate conditions. The radiocarbon dated stalagmite displays variations in winter climate, which seem to be strongly correlated with the winter NAO as reconstructed from tree rings and lake sediments (Trouet et al., 2009, Olsen et al., 2012, Ortega et al., 2015). Especially during the LIA the region received less precipitation in winter, with several short episodes of extreme dry events.

2. Site Description

The studied cave was formed within Variscan folded Upper Devonian to Lower Carboniferous limestone on the southern rim of the Fergana Basin in Kyrgyzstan (Fig. 1). About 15 km west from the city of Osh, close to the Uzbekistan border, the NW-SE directed mountain ridge Keklik-Too (Kirghiz for ‘secret’ or ‘cave mountain’) is located with 8.5 km length, 2 km width and a maximum altitude of 1,435 m above sea level (40°29’N, 72°35’E; Fig.1). The studied cave Bir-Uja, lies on the north-eastern mountain slope at about 1,325 m above sea level and has two entrances (Dudashvili and Dudashvili, 2012). The northern entrance is relatively large but is not accessible because it is located on a steep slope (Fig. 2). The chamber of the stalagmite location is overlain by about 30 to 50 m of limestone bedrock. A lot of stalactites but rare stalagmites are found in the cave. The cave floor is covered by red dust.

The mean annual air temperature is 12.1°C recorded between 1976 and 1996 at the meteorological station at the airport of Osh (875 m). Typical annual temperature and precipitation pattern (Fig. 1) corresponds to those of a summer warm continental climate. During summers precipitation is low and the region suffers from water deficit.

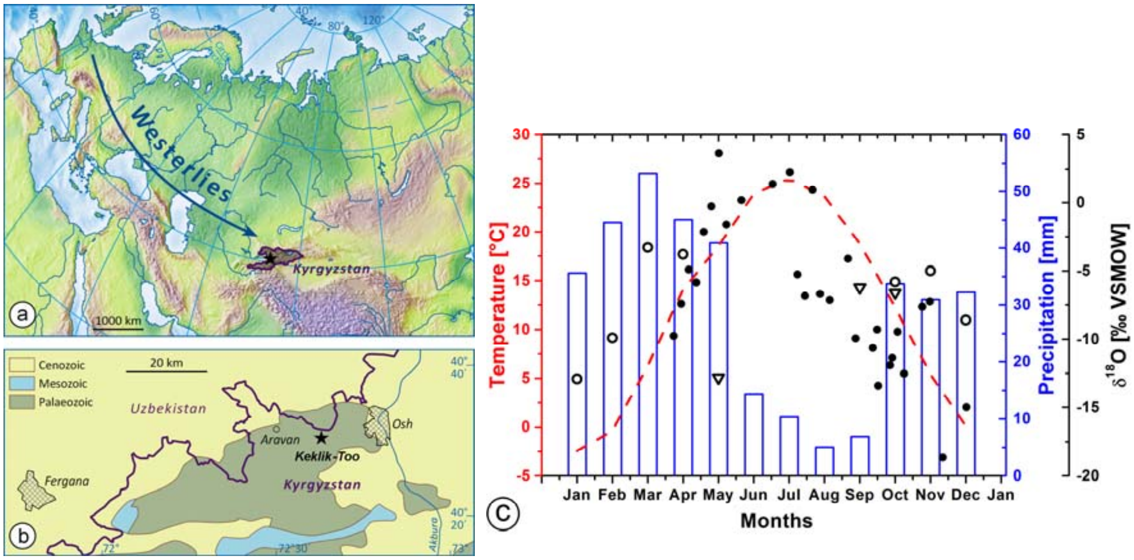

Fig. 1: a) Topographic map of Eurasia showing the principal track of Westerlies, b) Position of the Keklik-Too on the southern rim of the Fergana Basin and c) mean annual climate of Osh (temperature data (1977-1997) from *meteorological station GHCND:KG000038615*; precipitation *data (1967*-1993) are from *Global Historical Climatology Network accessed by the KNMI Climate Explorer), which is about 20km to the east of the cave. In addition, isotope data are shown for precipitation in Tashkent (300 km to the west of the cave) for 1971 (open circles, nearest Global Network of Isotopes in Precipitation station), for precipitation in Bishkek (300 km to the north of the cave) for 2001 (filled circles; Morris et al., 2005) stressing, that the annual cycle in the isotopic composition is consistent for the area of the cave. Cave drip water is represented by open triangles (see supplementary Tab. 1)*

The area above the cave is characterized by sparse vegetation and consists of montane grass and shrub lands, which change into bare rocks. The vegetation in this area is active in the spring season, but suffers from dry conditions during the summers. The cave itself is difficult to reach, which made it impossible to perform a regular cave monitoring. However, logged monitoring data for temperature and relative humidity (HUMILOG; Driesen&Kern) reveal that during the cold season from end of November to April, relative humidity in the cave is near 100% and temperature is around 12°C, which is close to the mean annual surface air temperature. With the beginning of the warm season in May, the cave temperature is gradually increasing up to 16.5°C while relative humidity declines from saturation to values between 70 and 60% and sometimes reaching only 40% (Supplementary Fig. 1). In September cave temperature is starting to decrease, while relative humidity starts to increase again in October. This behaviour implies a good cave ventilation during the warm season (May to November). Since a good cave ventilation usually is accompanied by a low cave air pCO_2 level (even close to atmospheric pCO2 levels; see e.g., Spötl et al., 2005; Frisia et al., 2011) we assume also a low cave air pCO2 in this season. In contrast, the cave air pCO2 level in the cold season (end of November to April) is expected to be significantly higher due to the poor ventilation, deduced from the high relative humidity. Consequently, carbonate precipitation and stalagmite growth must be most effective during the warm months. Evaporation effects, which are likely to occur in the warm, low relative humidity season, even can enhance carbonate precipitation (Deininger et al., 2012). Additionally, drip water was collected in spring 2012 and autumn 2011 and 2014 for stable isotope analyses. The host rock in caves, often acts as low pass filters with storing and mixing the rain from different seasons and any annual $\delta^{18}O$ signal in precipitation is strongly reduced (e.g., Riechelmann et al., 2011; Feng et al., 2014; Genty et al., 2014). Although only having three drip water samples available, the stable oxygen isotope composition (Fig. 1, supplementary Tab. 1), shows a large range of about 6‰, which is comparable to the range of $\delta^{18}O$ in regional, annual precipitation (Fig. 1; locations ~300km apart to the west and north). Thus, we deduce, that the potential to mix rain water in the overlying host rock and thin soil is low and that the rain water is not stored for longer than a few months in the host rock.

Stalagmite Keklik1 was removed in October 2011. The stalagmite grew about 40m away from the entrance (Fig. 2). The cave passage from the cave entrance A to the speleothem is relatively wide, so that the speleothem might be influenced by wind-transported dust and by kinetic fractionation effects if drip rate is low. Above the stalagmite formed a small ~5 cm long stalactite giving evidence for prior calcite precipitation. Observation of recent drip water suggests that the speleothem was still actively growing at removal. The stalagmite is about 135 mm long and well laminated. It is unlikely that the lamination represents annual layers. However, darker laminations may be related with longer phases of increased dust transport by wind. The high detrital content inhibits ^{230}Th dating as indicated by several analyses that provided ages with a huge uncertainty and which were completely out of stratigraphic order.

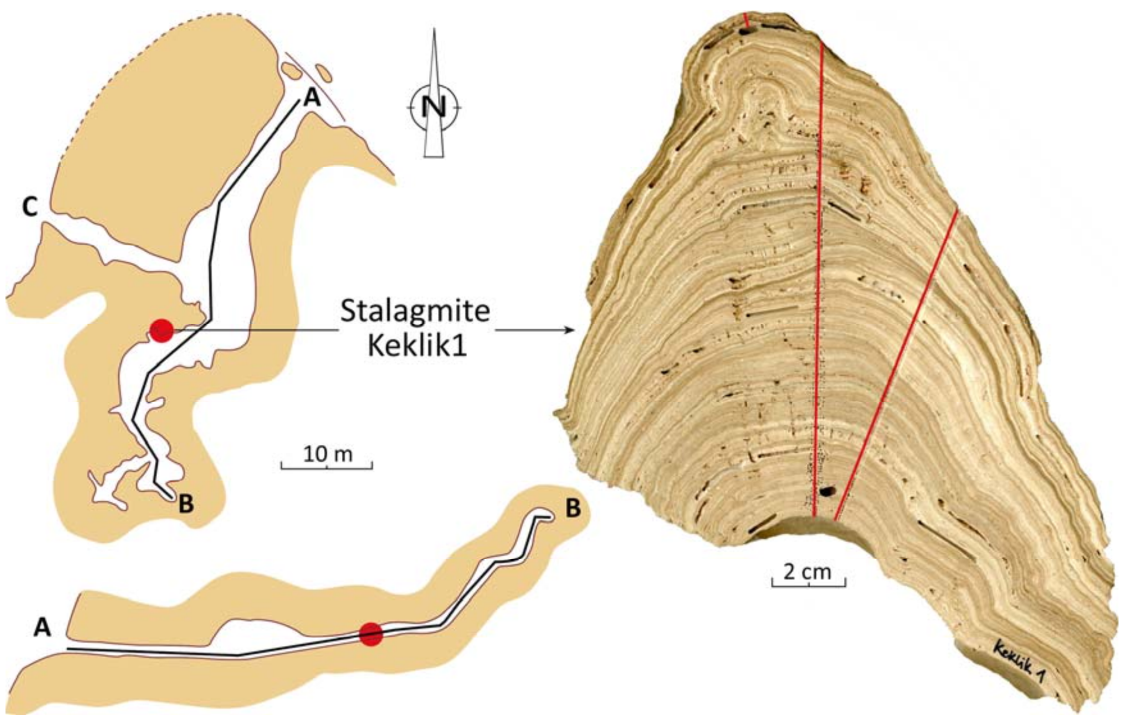

Fig. 2: *Plan view and profile of Bir-Uja Cave (modified after* Dudashvili and Dudashvilli, 2012*) with location and an image of stalagmite Keklik1. The cave has two entrances (A, C) but is only accessible through the eastern entrance (C). The stalagmite was found about 40 m from entrance A (dot). Stable isotope and μXRF element analyses of Keklik1* are *obtained from three sampling tracks (lines).*

3. Methods

3.1 Radiocarbon measurements

Seven samples for radiocarbon dating were drilled along growth layers of the stalagmite. Sample thickness is 2 mm and about 10 mg of carbonate were drilled in order to obtain 1mg of reduced C after sample preparation. Due to the well-laminated structure of the speleothem, the sample locations, which had partly to be drilled off the growth axis, could be well traced to the according depth at the growth axis. Sample depths are given with respect to its location at the growth axis (track 1).

Sample preparation and measurement was performed at the Poznan Radiocarbon Laboratory. The carbonate was hydrolysed with concentrated H_3PO_4 in a vacuum line. The obtained gas (CO_2 + water vapour) is then dried in a vacuum line, and reduced with hydrogen (H_2), using 2 mg of Fe powder as a catalyst. The obtained mixture of carbon and iron is then pressed into special aluminium holders (Czernik and Goslar, 2001). The IAEA C1 standard was used for background determination and treated in the same way as the samples. The ^{14}C content of a sample is determined using the spectrometer "Compact Carbon AMS" (National Electrostatics Corporation, USA). Detailed information about the measuring routine and protocols can be found elsewhere (Goslar et al., 2004). Conventional ^{14}C ages are corrected for isotopic fractionation using the $^{13}C/^{12}C$ ratio, measured simultaneously with the $^{14}C/^{12}C$ ratio by the AMS (Stuiver and Polach 1977). Errors are presented as standard deviation.

3.2 Stable isotopes

Three tracks for stable C and O isotope analyses were taken by micro-mil techniques using a Sherline 5410 milling machine. The right track was milled continuously at the flank of the speleothem while the central track was drilled along the growth axis and consists of two sections (Fig. 2). The tracks were measured at a resolution of 0.4 mm and 0.3 mm, respectively. Climate interpretation relies on the central track. Stable C and O isotopes were measured with an automated carbonate-extraction system (KIELIV) interfaced with a MAT253 IRMS (ThermoFisher Scientific) at the Helmholtz Centre Potsdam GFZ. Samples of around 60-90 µg were automatically dissolved with 103 % H_3PO_4 at 72°C and the isotopic composition were measured on the released and cryogenic purified CO_2. All isotopic ratios were expressed in the delta notation relative to VPDB. Replicate analysis of reference material (NBS19) reported relative to VPDB yielded standard errors of 0.06‰ for both, $\delta^{13}C$ and $\delta^{18}O$.

Water samples for stable isotope analyses of oxygen $\delta^{18}O$ and deuterium δD were collected from the stalagmite drip site at three occasions between October 2011 and September 2014 and were cool stored in sealed air-tight polypropylene bottles until analysis at the Alfred Wegner Institute for Marine and Polar Research in Potsdam. A Cavity Ring-Down Spectrometer (Picarro, L2120i) for water isotope analyses was used for determination of hydrogen and oxygen isotope composition, following (Meyer et al., 2000). Analytical precision of SMOW and SLAP calibrated analyses was better than 1‰ for δD and better than 0.3‰ for $\delta^{18}O$.

3.3 μXRF element scanning

Elements were analysed at the same tracks as the stable isotopes. The elements were measured by micro X-ray fluorescence (µXRF) techniques. Scanning was performed using an EAGLE III XL μXRF system spectrometer (Röntgenanalytik, Germany) at at the Helmholtz Centre Potsdam GFZ, applying a 40 kV tube voltage, a 300 μA tube current and 123 µm spot size. Sampling resolution of μXRF measurements was 50µm for the central track. The resulting data of this nondestructive method are intensities given in count per seconds (cps). The reproducibility was proven with multiple measurement runs along the same track indicating robust results for the elements, which are presented relative to calcium (element/Ca * 1000) to minimize variations, caused by sample geometry, physical properties and closed-sum effects along the measurement track.

4. Results

4.1 Radiocarbon chronology

Age control of stalagmite Keklik1 has to be obtained by means of radiocarbon dating, since detrital input to the stalagmite is too large to obtain reliable ages by ^{230}Th dating methods (the atomic

$^{230}Th/^{232}Th$ ratio is about 10^{-5}). The radiocarbon content generally decreases with depth except for the radiocarbon activity of sub-sample Keklik1-3c, which is slightly higher than Keklik1-11c. Such apparent radiocarbon age inversions are not uncommon in stalagmites, since it often suggests that radiocarbon reservoir variations occurred within the growth period of the speleothem (Tab. 1).

Tab. 1: *Radiocarbon activity of the samples from stalagmite Keklik1.*

Sample ID	Lab. no.	a14C [fm]	error [fm]	depth from top at growth axis [mm]
Keklik1-12c	Poz-67469	1.0979	0.0029	1
Keklik1-11c	Poz-67468	0.8677	0.0032	8
Keklik1-3c	Poz-64854	0.8742	0.0033	22
Keklik1-10c	Poz-66859	0.8618	0.0032	43
Keklik1-5c	Poz-64856	0.8586	0.0032	64
Keklik1-7c	Poz-64855	0.8169	0.0031	109
Keklik1-9c	Poz-66858	0.7889	0.0029	130.5

The upper radiocarbon measurement of Keklik1 provides evidence that the speleothem grew at least until the late 20th century. A radiocarbon signature of larger than 1 fm (fraction modern) is detected, which is only possible by transport of elevated atmospheric radiocarbon concentrations produced by tropospheric nuclear weapon tests in the middle of the last century. This finding supports the assumption of modern growth of the speleothem, as the drip location appeared active at time of stalagmite removal (Sec. 2). Leaving out the top radiocarbon value, we used six radiocarbon measurements for establishing the chronology.

For age-depth-modelling we follow the approach, proposed by Lechleitner et al. (2016). The common decay equation

$$A(t) = A(0)*\exp(-t/\tau), \quad (1)$$

(with time, t, radiocarbon life time, τ, and the radiocarbon activity, A) can be translated to a depth scale, d, assuming a sufficiently constant growth rate, GR, by t = d/GR. Using the logarithm of equation (1) and replacing t by d and GR results in

$$\ln(A(t)/A(0)) = -d/GR/\tau. \quad (2)$$

A linear fit is applied to the natural logarithm of the radiocarbon values over stalagmite depth. The slope, s, of this fit equals $1/GR/\tau$ and thus provides a direct estimate of the mean growth rate of the stalagmite. Using a point of known age, which for stalagmite Keklik 1 is the top of the speleothem (detection of bomb radiocarbon and actively dripping water on top of the stalagmite) it is possible to deduce on a first-estimate age control. So far this approach assumes, that the initial radiocarbon activity remained constant through time. Being well aware that this is unlikely due to the trends in the atmospheric radiocarbon concentration (Reimer et al., 2013), Lechleitner et al. (2016) proposed to use an iterative process to account for atmospheric radiocarbon variations. Starting with the age control from the first estimate age model, the atmospheric radiocarbon values (using IntCal13; Reimer et al., 2013) at the time of carbonate deposition can be used to correct for the variability of the initial radiocarbon concentration (A0) in the stalagmite. With the corrected radiocarbon activities, the fitting procedure is repeated, which results in a more accurate mean growth rate and a modified age-depth estimate than in the prior iteration. The new age model provides the possibility to perform a better correction of the initial radiocarbon activity by atmospheric radiocarbon values. The process is iteratively repeated until convergence of the mean growth rate is obtained, e.g., when growth rate is not changing by more than 1/1000 in successive iteration steps. For Keklik 1 this was reached after the fourth iteration. The corrected radiocarbon values are well represented by a straight line (Fig. 3). The remaining variability can be attributed to variability in the radiocarbon reservoir effect during C transfer dynamics from the soil to the cave. The approach predicts a mean growth rate of about 155+-14 µm/a for Keklik1 (Fig. 3).

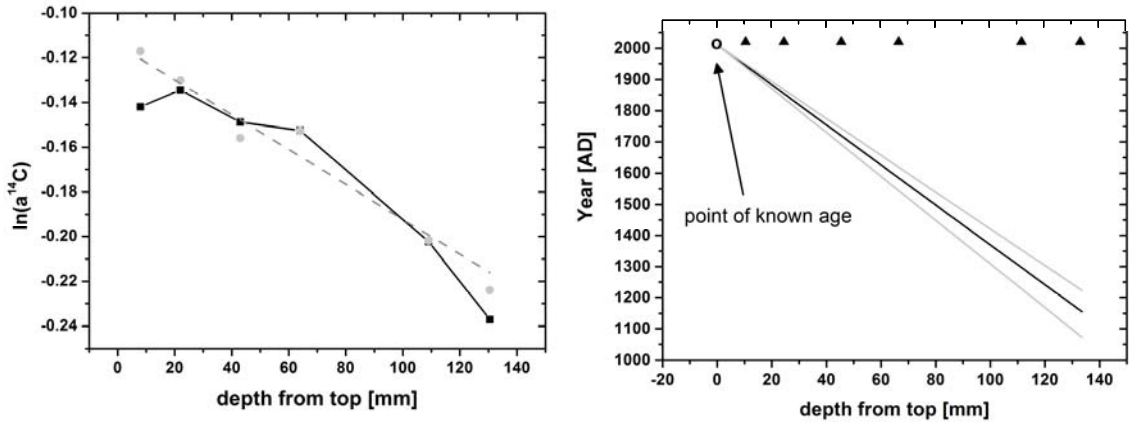

***Fig. 3: left:** Radiocarbon measurement points (black squares) are corrected for past atmospheric variations (grey circles) via IntCal13 (Reimer et al., 2013). Measurement errors are smaller than sign size. The corrected data can be well fitted (grey dashed line) by a linear correlation approach, which results in a value for r^2 of 0.96. This nearly perfect fit implies that the growth rate can be regarded as sufficiently constant over time.* ***right:** The growth rate is 155+/-14 µm/a. The time of stalagmite removal determines the end of growth and the age-depth model can be established (solid line) with the according uncertainty (grey). Triangles mark the positions of radiocarbon measurements.*

As deduced from the age modelling, Keklik1 grew between ~1150 AD and present day. Its growth appears to be continuous and was most likely not interrupted by periods of no-growth. Support for the established age model is provided by the S/Ca ratio (Supplementary Fig. 2). The beginning of the industrial revolution (~1750 AD) led to increased fossil fuel burning, which resulted in massive injections of S to the atmosphere. Finally, the S aerosol particles were washed out by precipitation and reached the stalagmite. As a result, the S/Ca ratio of Keklik1 increases remarkably at this time and remains at high values.

4.2 Stable C and O isotopes

Stable C isotope values range from -7.6 to +0.5‰ (Fig. 4b). Between about ~1150 AD and ~1450 AD the C isotopic composition decreases from values around -5.5‰ to values about -6.5‰. In this period the variability is relatively small, compared to the following period. A weak trend towards a higher stable C isotopic composition is observed until around ~1700 AD. By the end of this period, $\delta^{13}C$ values of about -5‰ are observed. Between approximately ~1600 and ~1850 AD large positive C isotope anomalies occur frequently with maximum values up to +0.5‰. Within the last ~150 years a slight increasing trend towards values of -4.0‰ is present and variability of the stable carbon isotope composition is smaller than in the period before.

Stable O isotopes (Fig. 4c) show the same general pattern as $\delta^{13}C$. In the period between ~1150 AD and about 1450 AD the mean $\delta^{18}O$ values decrease from -10.5 to -11.5‰ with small internal variability compared to the following period between approximately ~1450 and ~1850 a BP. During this period the mean $\delta^{18}O$ carbonate composition increases to about -10‰ with strong positive anomalies up to -5.5‰. Thus, the total spread of the stable O isotopes spans a very broad range of 7‰ (between -12.5 to -5.5‰), similar to the recently studied speleothem Uluu-2 from a cave nearby (Wolff et al. 2017).

Both, $\delta^{13}C$ and $\delta^{18}O$ are well correlated - especially at the positions of the positive isotope anomalies. The largest anomalies (by isotope range and duration) are centred at about ~1520, ~1600, ~1735 and ~1815 AD. However, also towards the end of the stalagmite growth period, both isotope systems show a strong positive anomaly. A 15-point running correlation calculation clearly shows that during large parts of stalagmite growth $\delta^{13}C$ and $\delta^{18}O$ vary nearly perfectly (Fig. 4d). The correlation coefficient is often near 1 and in about 66% of the isotope data statistically significant above the 99% level.

The slope between $\delta^{13}C$ and $\delta^{18}O$ of the 15 points used for the correlation calculation is also computed within a 15-point running window (Fig. 4e). It is very interesting to see that for most periods, where the correlation coefficient shows large values, the slope between $\delta^{13}C$ and $\delta^{18}O$ has also high values (often > 1). Only for very short intervals, the 15-point running correlation coefficient and the according slope are negative, but not statistically significant above the 99 % level.

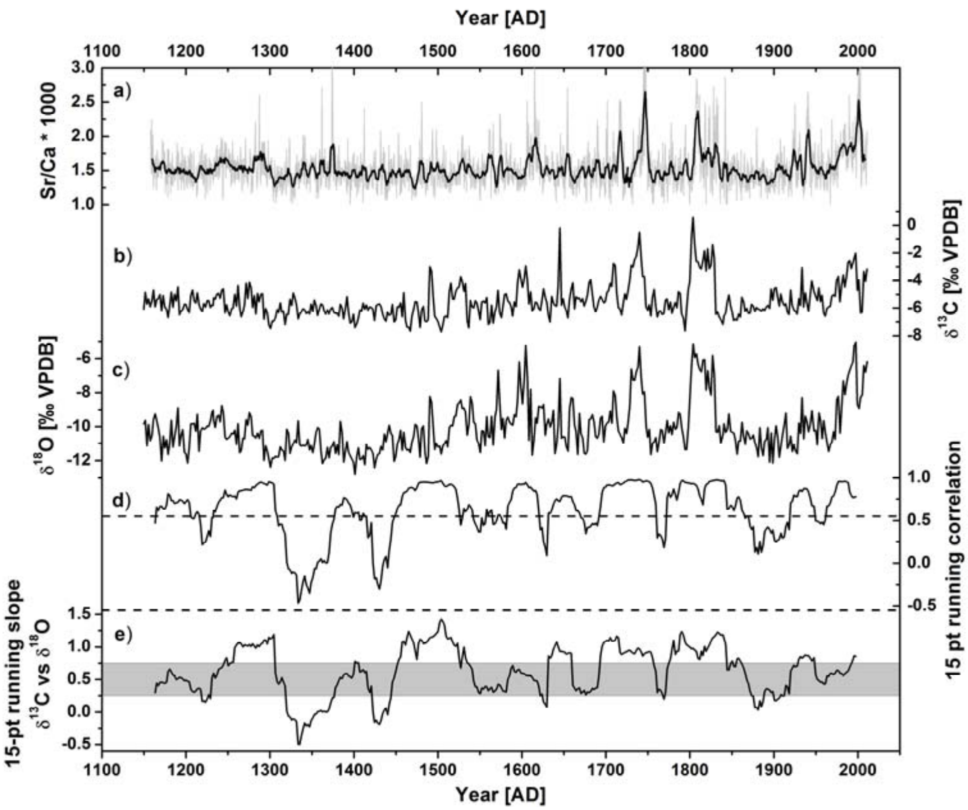

Fig. 4: *The Sr/Ca ratio (a) shows strong peaks, which are simultaneous with the positive stable isotope anomalies (grey: original data; black: 15-pt running mean). The stable C (b) and O (c) isotope composition of Keklik1 show strong variability and a strong coherence. This is supported by high values for the 15-pt running correlation coefficient (d) of both proxies. For about 2/3 of the time series the correlation is above the 99 % significant level (upper dashed line). The correlation coefficient is never below the negative 99 % significant level (lower dashed line). The corresponding 15-pt running slope between* $\delta^{13}C$ and $\delta^{18}O$ *values (e) shows a large variability and often exceeds the experimentally*

found range (grey shaded rectangle) determined by laboratory experiments (Wiedner et al., 2008, Polag, 2009, Polag et al., 2010, for more details see Sec. 5.2).

4.3 Element data

This study focusses on Sr/Ca ratios since these are often regarded as a suitable proxy for infiltration of rainfall (Fairchild and Treble, 2009). Normalisation of Sr element counts with the Ca counts minimizes the effects caused by variations of the sample geometry (e.g, holes) and physical properties of the speleothem. Reliable measurements were not obtained at depths with large holes on the speleothem surface. Therefore, a few gaps appear within the measurement track. The Sr/Ca record reveals rather constant background values with strong peaks indicating an increase by a factor of two (Fig. 4a). Short-term fluctuations in the Sr/Ca record with higher values match well with the course of the stable isotope values (Fig. 4a). However, long-term trends as described for the stable isotopes are not present in the Sr/Ca record.

5 Discussion

5.1. Chronology

Radiocarbon dating of secondary carbonates is not straightforward. A priori unknown reservoir effects are responsible for obtaining older radiocarbon ages compared to the time of growth. Soil gas CO_2, with a radiocarbon composition similar to or slightly lower than that of the atmosphere, is dissolved by infiltrating rainwater. The resulting carbonic acid dissolves the radiocarbon free carbonate of the host rock after the soil water enters the epikarst. Depending on the carbonate dissolution process (Hendy, 1971) up to 50 % of C dissolved in water can have its origin from the radiocarbon free host rock. That would require carbonate dissolution under closed conditions. Those conditions occur when the water dissolving the host rock is not in contact with soil gas and, thus, gas exchange of dissolved carbonate species with gaseous CO_2 is impossible. In case the water, which dissolves the host rock, is in contact with soil gas C, exchange between the dissolved carbonate species and gaseous CO_2 occur and the dissolved inorganic carbonate is in isotopic equilibrium with soil gas CO2. Hence, the radiocarbon reservoir effect can contribute between 0 years and one radiocarbon half-life (5730 years). Additionally, the reservoir effect is unlikely to be constant over time. More details about the carbon transfer dynamics and processes, which might lead to changes in the radiocarbon reservoir effect can be found elsewhere (Genty et al., 2001; Fohlmeister et al., 2011a; Rudzka et al., 2011; Griffiths et al., 2012).

Despite those difficulties there are approaches used to obtain reliable age-depth relationships with radiocarbon (Rudzka et al., 2012; Hua et al., 2012). However, all those approaches require a precise knowledge of the radiocarbon reservoir effect and have to assume that the reservoir effect is sufficiently constant. Nevertheless, recently Lechleitner et al. (2016), put more effort into establishing radiocarbon based age-depth relations in speleothems. Adapting the methodology of marine sedimentology derived ^{230}Th-excess dating they propose a new approach to use a set of radiocarbon ages for age-depth control in speleothems. Advantageously, the new approach does not require any knowledge about the magnitude of the radiocarbon reservoir effect. Additionally, this approach is also independent of reservoir effect variations as long as long-term trends in the reservoir effect over the whole speleothem are absent. Since the reservoir effect can depend on hydrologic characteristics (e.g., Fohlmeister et al., 2010; Griffiths et al., 2012), trends in the reservoir effect are often accompanied with trends in other hydrological proxies ($\delta^{18}O$, Mg/Ca, Sr/Ca or $\delta^{13}C$). No long-term trend in any proxy of Keklik1 is observed (see Sec. 4.2 and 4.3), which allows to assume that the radiocarbon reservoir effect does not show a non-stationary behaviour. This enables us to apply this approach. Note, that short-term variations in the reservoir effect do not influence the result. However, we like to emphasize that this modelling approach works best, when growth rate is sufficiently constant, as it can give only a linear approximation of the growth history. Major changes in growth rate cannot be detected. This should be kept in mind, when comparing the timing of climate events inferred from this stalagmite to other archives.

5.2 Proxy interpretation

Sr/Ca element ratio

Annual changes of the Sr/Ca ratio often reflect seasonal variability of the growth rate induced by seasonally different cave ventilation (e.g., Huang et al., 2001; Huang and Fairchild, 2001; Stoll et al., 2012). However, the mean annual growth rate of Keklik1 is approximately 155 µm (see Sec. 4.1) and therefore annual variability in Sr/Ca cannot be accurately captured by the µXRF scanning resolution of 50 µm. On longer time scales, the ratio between Sr and Ca is frequently regarded as a proxy for infiltration amount of meteoric water (e.g., Treble et al., 2003; Cruz et al., 2007; Fairchild and Treble, 2009). Prior calcite precipitation, a process, which is more pronounced during periods of low water infiltration, elevates the Sr/Ca ratio by preferential precipitation of Ca^{2+} compared to the metal.

The Sr/Ca record has a relatively constant baseline, which suggests that no long-term trend in precipitation occurred during the last about 900 years. However, frequent positive anomalies give evidence for short periods of 5 to 30 years with strongly reduced infiltration. The Sr/Ca ratios suggests that the low-infiltration events occurred around ~1600, ~1735, ~1815 and ~1940 AD as well as in the last years of speleothem growth (Fig. 4). The occurrence of these dry events is more often and appear to be stronger during the last 400 years compared to the period before.

The knowledge of the cave processes (see Sec. 2) allows to deduce in even more detail, in which season the precipitation decreased during the dry events. The host rock and soil above the cave are thin and water seems to penetrate fast through those horizons. In addition, cave ventilation is responsible for enhanced air exchange between cave and atmosphere during the warm season, leading to increasing temperatures in the cave and decreasing relative humidity values (~60%;

supplementary Fig. 1). These conditions imply low pCO_2 values in cave air and a large difference between dissolved CO_2 in water and CO_2 in cave air. Consequently, this favours carbonate precipitation in the warm season, while in the cold season carbonate precipitation is limited because a smaller pCO_2 difference between drip water and cave air exist. Those seasonal calcite precipitation pattern are amplified by the Ca^{2+} concentration in the drip water, which is about ten times lower during the cold season (supplementary Tab. 1). The low amount of Ca^{2+} in drip water during the winter mode reveals that winter precipitation is not able to dissolve much carbonate. This can be explained by limited amounts of biogenically derived soil gas CO_2 in the cold season (e.g., Spötl et al., 2016). Due to the low vegetation density of the grass land and thin soil above the cave, soil respiration rate in the non-growing season (winter) is expected to be small (e.g., Schlesinger 1977; Parker et al., 1983). This leads only to a small enrichment in soil gas CO2 compared to atmospheric CO_2 concentrations (Cerling, 1984). Another explanation might be the fast penetration of winter precipitation, which might be too fast to dissolve large amounts of the epikarst carbonates. Therefore, both, cave ventilation and carbonate dissolution, provide more favourable conditions for carbonate precipitation and stalagmite growth during the warm season. In contrast, the potential for carbonate precipitation in winter is limited for this cave

As the warm season is the main important growth period, it is now important to discuss the season of the drip water, which is arriving the cave in summer. Summer precipitation is generally low (Fig. 1) and increased evapotranspiration causes no or nearly no rain from this season to penetrate through the soil and host rock. Thus, the amount of infiltrating cave water appears to be negligible during the warm season months of June to September. However, as explained in Sec. 2, the soil residence time of water is short. Therefore, spring precipitation, moving a few months through the karst, is one source of warm-season cave drip water. A second potential source might be winter snow, which is melting in spring. Usually, snow melts away in February/March (supplementary Fig. 4) and enter the cave enters the cave, when the cave system turns into its warm season mode, when the potential for carbonate precipitation is highest. Autumn precipitation does not seem to affect stalagmite growth, because water transition time through the epikarst is short, such that those waters enter the cave in the cold season, where carbonate precipitation is most likely not very high (see Sec. 2). Thus, the Sr/Ca ratio of stalagmite Keklik1 is a tracer for the amount of precipitation during the winter and spring season.

Albeit wet, also warm winters can contribute to elevated Sr/Ca ratios. During warm winters, precipitation may occur more often as rain or snow melts earlier (Aizen et al., 1997; Khalsa and Aizen, 2008; Sorg et al., 2012). For the last 17 years, important snow melt events occurred even in the middle of the winter, as present-day satellite data for the last 17 years demonstrate for this region (see supplemental Fig. 4). Then winter rain immediately penetrates into the soil and epikarst and enters the cave, when it is still in its cold season mode. This way, winter precipitation is also not able to efficiently contribute to speleothem growth. As since the 1970ies a winter warming trend for the region around the cave is observed (Fig. 5), the Sr/Ca ratios of the stalagmite show also an increasing trend during the last 40 years (Fig. 5). This is interpreted to reflect rather warm winter temperatures and not low precipitation conditions during winter and/or spring.

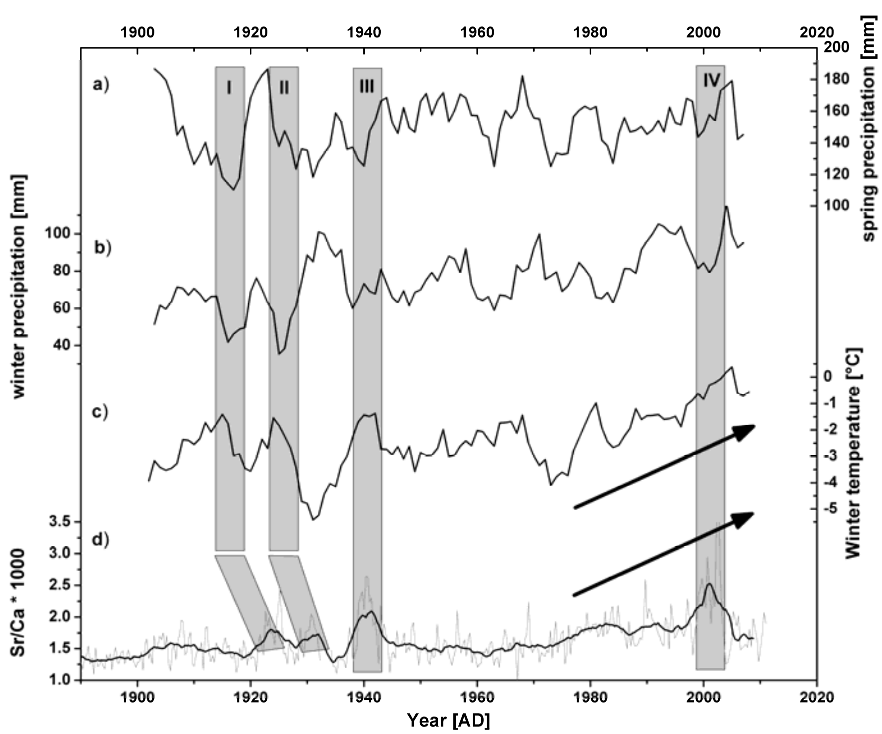

Fig. 5: *Gridded reanalysis data of a) spring (MAM) and b) winter (DJF) precipitation, c) winter (DJF) temperature at the cave location as well as five year running mean of d) Sr/Ca ratio (raw data in grey). Grey boxes represent positive Sr/Ca anomalies (less precipitation). The increase in Sr/Ca ratio after about 1970 AD is due to the winter warming (black arrows) in the cave region. Grey rectangles mark periods (I to IV) of positive Sr/Ca anomalies. Non-synchrony of events (inclined rectangles) may be a matter of the speleothem age uncertainty. Precipitation (Schneider et al., 2011) and temperature data (Willmott, C. J. and Matsuura, K., 2001) are provided by the NOAA/OAR/ESRL PSD, Boulder, Colorado, USA, from their web site at* http://www.esrl.noaa.gov/psd/.

Most of the Sr/Ca extreme events must be explained differently than the recent increasing Sr/Ca trend observed over the last 40 years. The winters during anomalies I and II (as defined in Fig. 5) were relatively warm, and coincide with low amounts of precipitation in winter and spring, which results in increasing Sr/Ca values. Period III (Fig. 5) was also relatively warm during winter, but winter precipitation appeared normal. However, under those warm winter conditions most likely the precipitation was more often falling as rain and the snow was melting early as observed for the most recent years (supplementary Fig. 4). Spring precipitation is low, which in concert with the warm winters is responsible for an increase in the Sr/Ca ratio. The last Sr/Ca peak in period IV is due to the exceptionally warm winters and the relatively low precipitation in spring. There are also other periods of warm winters as in the late 1960ies or around 1980 AD. However, both periods have had also high amounts of spring precipitation. Therefore, the Sr/Ca ratio did not increase much at those times.

Stable isotopes

Contemporaneously occurring variations in C and O isotope composition are usually a hint on kinetic isotope fractionation effects (e.g., Hendy 1971, Mickler et al., 2006). The strong correlation between $\delta^{18}O$ and $\delta^{13}C$ (Fig. 4d) over the whole Keklik1 record suggests that drip rate related fractionation changes or kinetic effects are important for the isotope signal. Especially, during the dry events, as derived by the Sr/Ca ratio, the positive anomalies in the stable isotopes might be controlled by fractionation effects during carbonate precipitation in the cave. The 15pt running correlation coefficient is significant for about 66% of the whole time series and even close to 1 at and around the dry events. In the scope of fractionation controlled isotopic composition of the stalagmite, it is interesting to analyse the slope between $\delta^{13}C$ and $\delta^{18}O$ (Fig. 4e). During periods, where the correlation coefficient is near 1, the slope between $\delta^{13}C$ and $\delta^{18}O$ (X vs Y) is also near and even above 1. Such values are extremely large when compared to laboratory and cave experiments, which have investigated stable isotopes along the path of carbonate precipitation (Mickler et al., 2006; Wiedner et al., 2008; Polag, 2009; Polag et al., 2010). Also studies, which investigated correlation coefficients between both stable isotopes for short periods along the growth axis of stalagmites, only rarely obtained values above 1 for the slope (Mickler et al., 2006; Boch and Spötl, 2011). The slopes found in cave and cave analogue laboratory experiments are in the range of 0.25 to 0.75 (supplementary Tab. 2). Larger slopes, as detected for most parts of Keklik1, thus, mean that changes in $\delta^{18}O$ of the carbonate are not only due to fractionation but must be influenced by at least one additional process. The most likely process is that $\delta^{18}O$ of infiltrating water could have been changed. Potentially, this can happen as a result of a changing seasonality of precipitation, i.e. changes in the amount of winter compared to spring precipitation or changes in the isotopic composition of precipitation itself.

This means that at least two major factors control $\delta^{18}O$ of Keklik1: in-cave fractionation and isotopic variations in meteoric water. In-cave fractionation processes show a constant relationship between $\delta^{13}C$ and $\delta^{18}O$. Along individual growth layers, correlation coefficients are close to 1 and the slope between $\delta^{13}C$ and $\delta^{18}O$ (X vs Y) is relatively constant between 0.25 and 0.75. This finding can be used to correct the stable O isotope signal for fractionation processes between drip water and carbonate.

For this purpose, it is assumed that the whole short-term variability of the $\delta^{13}C$ values is due to fractionation. Thus, this approach gives an upper limit for the fractionation induced changes in $\delta^{18}O$. Before the correction is applied, the weak long-term trends of the $\delta^{13}C$ and $\delta^{18}O$ time series are removed by subtracting a best fit polynomial of third order. The origin of the long term trend might be related to changes in the isotopic composition of winter and/or spring composition itself. A more detailed discussion about the long-term trend is given in Sec. 5.3. Correction calculations for the fractionation effects in the $\delta^{18}O$ signal are then performed with the mean, previously observed value for the slope between $\delta^{13}C$ and $\delta^{18}O$, which is 0.5. This means: if the variation in the (long-term trend reduced) $\delta^{13}C$ signal due to fractionation is approximately 4‰, then the corresponding $\delta^{18}O$ variation, which can be ascribed to fractionation, is about half as large, i.e. 2‰. Applying this approach for the whole record, the measured $\delta^{18}O$ signal is reduced to a $\delta^{18}O$ signal, which is corrected for in-cave fractionation processes. The resulting in-cave fractionation corrected $\delta^{18}O$ values then represent the pure drip water oxygen isotope signal. This signal has a lower range (about 2 to 3‰) than the original time series, but the shape is similar (Fig. 6).

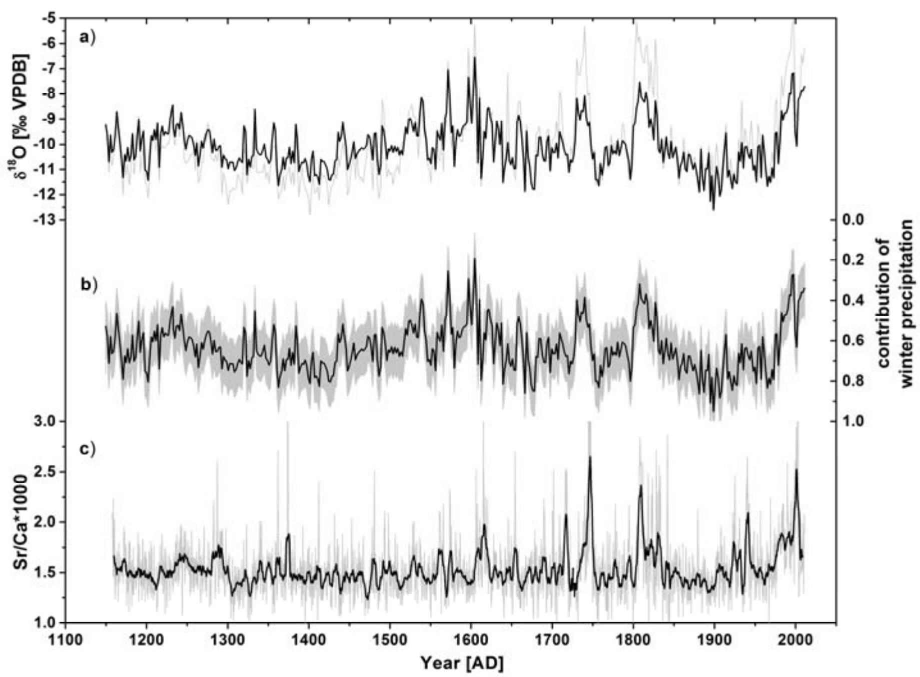

Fig. 6: *a) A comparison of original (grey) and for fractionation processes corrected* $\delta^{18}O$ *of speleothem calcite (black) reveal the strong influence of fractionation on the original time series. However, the influence of seasonality in the corrected time series is also large with up to a range of ~3‰. b) The*

corrected $\delta^{18}O$ values allow to compute the relative contribution of winter precipitation to the carbonate and error envelope (see text and supplementary material for details; axis reversed). When winter contribution is reduced, the Sr/Ca ratio (c) recorded dry events, implying that indeed the amount of winter precipitation is reduced instead of an increasing amount of spring precipitation.

Strong support for the correction procedure is derived from the interpretation of the Sr/Ca ratio. During periods of elevated Sr/Ca ratios, which represent dry phases, the strongest isotope correction was obtained. This is in line with the usual interpretation of changes in the strength of enrichment in the $\delta^{18}O$ isotope composition of speleothems. Usually a stronger enrichment is expected under dry, low drip rate conditions (Mühlinghaus et al., 2009; Dreybrodt and Scholz, 2011; Deininger et al., 2012).

After removing the influence of fractionation in the cave, it is possible to disentangle the relative contribution of winter to spring precipitation by using the differences in the isotopic composition in meteoric precipitation in both seasons (Fig. 1). For this purpose, in first order, it is assumed that the O isotope composition of winter and spring precipitation did not change considerably during the last about 900 years and was nearly constant at present day mean values of -13‰ for the winter months and about -5‰ during the spring season (Fig.1). Then, it is possible to compute the relative proportion of each season's precipitation to the fractionation corrected $\delta^{18}O$ signal of Keklik1 (Fig. 6b). We want to emphasize, that for the fractionation corrected $\delta^{18}O$ record, we have removed a long term trend from the measured $\delta^{18}O$ record. This long term trend might be a result of changes in the isotopic composition of precipitation itself as the sources of precipitation might have been changed (North Atlantic/Eastern Mediterranean/Black Sea) or of temperature induced changes in the strength of fractionation (see Sec. 5.3). On short-term, changes in the $\delta^{18}O$ composition of winter and spring precipitation are also relatively likely and cannot be easily corrected for. For this reason, we estimated an uncertainty for the reconstruction assuming an arbitrarily chosen variation in mean winter and spring precipitation of +/- 1‰. Also sublimation of snow might lead to some minor enrichment in the infiltrating water, compared to its original composition. It was shown, that this effect is more important for dry winters as for wet winters, as only the surface of the snow cover is subject to an enrichment in the isotopic composition (Stichler et al., 2001; Vuille et al., 2003). During exceptionally dry winters, as interpreted for the periods of the strong positive anomalies, thus sublimation may lead to somewhat enriched $\delta^{18}O$ values of melting snow and to some amplification of the strong $\delta^{18}O$ anomalies.

Since the corrected $\delta^{18}O$ signal was calculated with the total range of $\delta^{13}C$, the derived seasonal variation of precipitation, which has arrived the cave in its warm season mode (Fig. 6b), must be considered as a minimum estimate. It might be possible that not the whole range in $\delta^{13}C$ is due to in-cave fractionation processes. Then the total range of the season’s precipitation contribution would be enlarged, but, the shape of the corrected $\delta^{18}O$ signal would remain similar. Reasons for $\delta^{13}C$ to vary, can originate from changes in the isotopic composition of soil gas $\delta^{13}C$ due to changes in vegetation density (Cerling, 1984), water stress of plants (Buchmann et al., 1996; Bowling et al., 2002; Hartman and Danin, 2010) or carbonate dissolution (Fohlmeister et al., 2011b). The direction of change would coincide with the tendency, obtained by drip rate related changes during fractionation processes in the cave.

The reconstruction reveals that the relative winter contribution with respect to spring precipitation is mostly between 60 to 80%. Large deviations from this range are observed between ~1550 AD and ~1850 AD. According to the interpretation derived above, the two explanations for winter precipitation reductions include (I) relatively warm winters or (II) low amounts of winter precipitation. Since these periods of a low contribution of winter precipitation occurs throughout the period of the LIA, a period which is known for cold winters in Europe (e.g., Wanner et al., 2001; Grove, 2004; Holzhauser et al., 2005; Fohlmeister et al., 2012; Schimmelpfennig et al., 2014) and Western and Central Asia (e.g., Esper et al., 2002; Sorrel et al., 2007) it is most likely, that the positive $\delta^{18}O$ anomalies point to a low amount of winter precipitation. Those dry winter events lasted often approximately 5 to 30 years and the contribution of winter precipitation was reduced to about 30%.

Nowadays, the stable oxygen isotopic composition is also comparable to those dry winter periods in the LIA. However, in contrast to the LIA, the reason for the elevated $\delta^{18}O$ and apparently low contribution of winter precipitation in the carbonate of Keklik1 in the last about 40 years originates rather in the relatively mild winter conditions during the present warming period (Fig. 5c).

5.3 Is winter NAO controlling the precipitation pattern?

Evaluating the isotopic and Sr/Ca changes of the Keklik1 stalagmite revealed that the distribution of winter-spring precipitation plays a dominant role during stalagmite growth. The lack of highly resolved winter/spring precipitation records spanning the last millennium hamper a proper comparison of the Keklik1 record with other local climate records. Nevertheless, when opposing our Keklik1 record to a winter precipitation record from a location ~300km to the southeast (Aichner et al., 2015) and a composite annual precipitation reconstruction, which is centred about 500 to 1000 km to the east (Chen et al., 2010) an opposite relation for precipitation can be observed (Fig. 7). In phases, where our Keklik1 record indicate lower amounts of precipitation (especially during the LIA), both other records suggest higher amounts of annual and winter precipitation. The opposite behaviour is observed during the MCA. Both other studies relate their precipitation record with respect to the intensity of westerly winds and precipitation brought with them. Their finding was supported by comparison of their records to NAO reconstructions (Trouet et al., 2009; Olsen et al., 2012). The negative Central Asia winter precipitation vs. NAO relationship is supported by meteorological observations from stations throughout Central Asia (Aizen et al., 2001). However, this link is not supported by other paleolimnological climate records that suggest a positive connection between both parameters during the Mid- to Late Holocene (e.g., Huang et al., 2011; Lauterbach et al., 2014; Taft et al., 2014).

Here, we use for comparison purposes the most recent NOA reconstruction by Ortega et al. (2015) (Fig. 7), which is based on 48 annually resolved proxy records. Between ~1400AD to present the reconstruction is similar to the reconstruction provided by Trouet et al. (2009) but in contrast to Trouet et al. (2009) the new reconstruction shows no persistent positive NAO phase during the medieval period. Instead, the Ortega et al. (2015) record suggests that positive phases were only dominant during the thirteenth and fourteenth centuries. Comparison of the Keklik1 $\delta^{18}O$ record and the NAO index reconstruction of the last millennium (Ortega et al., 2015) suggests a positive relationship (Fig. 7). Both records have the same features - although with imperfect timing - when considering, that the radiocarbon derived age-depth model cannot be as precise as the annually resolved NAO reconstruction. The offset in the timing between higher $\delta^{18}O$ values and a negative NAO index can be ascribed to slight variations in the growth rate of the stalagmite, not captured by the age model.

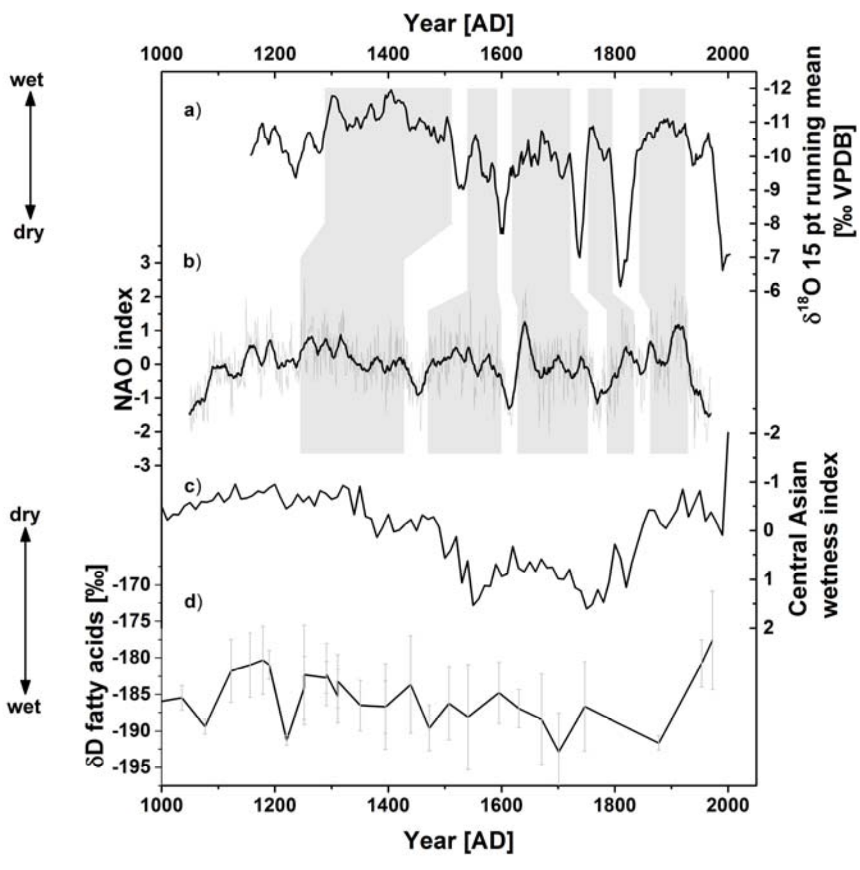

Fig. 7: The Keklik1 $\delta^{18}O$ time series (a) compares well with the NAO index (b; Ortega et al., 2015). Each strong negative NAO phase during the LIA can be attributed to a period of significantly reduced

winter precipitation (high values in $\delta^{18}O$, white space between grey bars). Please note, that the radiocarbon based age model of Keklik1 is not as precise as the 48 annually resolved proxy records used for the NAO reconstruction of Ortega et al. (2015). An opposite behaviour between NAO and Central Asian precipitation is observed for more south-eastwards located records: c) a composite Central Asian wetness index (with archives spread in Central Asia and centred ~ 500-1000km to the east of our location; Chen et al., 2010) and d) the deuterium isotopic composition of C26 and C28 fatty acids from Lake Karakuli (~300km to the south-east; Aichner et al., 2015).

Positive winter NAO conditions, which prevailed during the MCA, are related to light stable oxygen isotope composition in precipitation based on the Keklik1 data set and vice versa (Fig. 7). More depleted oxygen isotope ratios suggest a steady and high amount of winter precipitation in form of snow. The characteristic directions of westerly winds and distribution of precipitation for positive and negative NAO phases provide a possible teleconnection mechanism between the North Atlantic sector and Central Asia and can explain the observed changes. Positive NAO anomalies cause a strengthening of the westerly winds over Central and Northern Europe (e.g., Wassenburg et al., 2016) heading on a northern trajectory towards Central Asia. Such positive NAO modes generally weaken the Siberian High (e.g.; Gong et al., 2001; Gong and Ho, 2002) and prevent dry and cold Arctic air from reaching Central Asia and the Tian Shan region. This results in relatively wet winters in the western Tian Shan. These conditions appear relatively stable throughout the MCA since no strong short-term variations in $\delta^{18}O$ or Sr/Ca are observed. Negative NAO anomalies causes a southward shift of the westerly winds and head over southern Europe towards Central Asia on a more southern trajectory than during phases of a positive NAO index. This allows cold and dry Arctic air steered from the Siberian High to reach far southwards into Central Asia (Wanner et al. 2001; Folland et al., 2009, Seyd et al., 2010) leading to dry winters at our cave side.

The explanation provided for the Keklik1 location is very likely also valid for more western (Lake Aral; Huang et al., 2011) and northern situated records (Lake Son Kul; Lauterbach et al., 2014) as they observe also a positive relation to NAO. However, this argument seems to be invalid for the records located to the east and south-east with respect to our location, since those records (Aichner et al., 2015; Chen et al., 2010) show a negative relationship with the NAO index (Fig. 7). We hypothesize that the mountains of the Tian Shan and Pamir form a natural barrier for the westerly winds. During positive NOA phases, when winds are directed over central and northern Europe towards Central Asia, they are likely to be re-directed to the north once they reach the Tian Shan and Pamir. Therefore, they cannot provide precipitation for the southern and eastern part of Central Asia. However, during negative NAO phases, when westerly winds are heading on a more southern trajectory towards Central Asia, the westerly winds seem to be able to contribute to winter precipitation in southern and eastern Central Asia.

As discussed above, the short-term excursions in $\delta^{18}O$ of Keklik1 appear to be linked with the contribution of winter precipitation. In contrast, the long-term trend in the Keklik1 isotope data cannot be explained in this way, because there is no similar long-term trend in the Sr/Ca ratio. However, the NAO modes are also thought to govern temperature changes over Northern Eurasia. Positive phases seem to enhance advection of warm air over central and northern Europe and the western or even central part of north Asia (Hurrell and Van Loon, 1997; Thompson et al., 2000). This weakens the Siberian High, which cannot expand during those conditions. As such, a positive NAO mode could likely not only lead to warmer winter conditions in northern Europe (Hurrell, 1996) but also in Central Asia. This might be the predominant climate state during the MCA, where the reconstructed NOA index was generally more positive (Fig. 7; Ortega et al., 2015). Subsequently, climate runs into a period with phases of a more negative NAO index causing a climate deterioration known as the LIA. As a result, the Siberian High is becoming more important for Central Asia (e.g.; Gong et al., 2001; Gong and Ho, 2002) and winter temperatures would decrease. Those temperature variations occurred not exclusively in winter, but also in the warm season as shown by tree ring reconstructions from the Tian Shan region (Esper et al., 2002; 2003). Variations in surface air temperatures would cause changes in cave temperature as cave monitoring revealed that carbonate precipitation occurs during the warm season months, when the cave temperature is sensitive to the outside air conditions (supplementary Fig. 1). This, must have induced a change in O isotope fractionation during carbonate precipitation, and might explain the long-term trends in the stable O isotope records. Thus, in cold climate phases (e.g., during the LIA) isotope fractionation effects must have been larger, leading to more enriched $\delta^{18}O$ values in the carbonate, compared to the $\delta^{18}O$ values observed during predominantly warm phases (e.g., MCA).

Alternatively, the isotopic composition of precipitation was changing with time and lead to the observed long-term O isotope variations. Especially, for winter conditions this could be a valid argument. The isotopic composition of precipitation is certainly different when arriving from predominantly western locations during positive phases of NAO compared to phases of a negative NAO, when the source of precipitation is more dominated from the Siberian High.

In contrast to the $\delta^{18}O$ long-term trend, the long-term variation of the $\delta^{13}C$ time series needs an additional process, since temperature related changes in $\delta^{13}C$ fractionation processes are too small to explain the $\delta^{13}C$ range observed in the stalagmite and the origin of precipitation is not important. Most likely, changes in vegetation also contribute to the long-term trend. Warmer and wetter periods are favourable for plants and thus, would result in a denser vegetation cover and in higher soil respiration rates (e.g., Cerling 1984). Both are responsible for a lower C isotopic composition of soil gas CO_2, which signal is stored in the C isotope composition of the speleothem.

6. Conclusions

We dated a stalagmite from the Keklik-Too in western Kyrgyzstan by means of a newly proposed dating approach based on radiocarbon measurements. This age-depth-modelling approach is independent from the knowledge of the radiocarbon reservoir effect or its variations. The method provides an accurate estimate of the growth history of this stalagmite, which cannot be dated by means of ^{230}Th methods due to a high detrital component.

We have demonstrated that stalagmite Keklik1 from the Keklik-Too in western Kyrgyzstan has interesting characteristics in terms of cave processes and speleothem growth. Those processes allowed interpretation of the stalagmite proxies in terms of climate. Sr/Ca, δ^{18}O and δ^{13}C have simultaneous peaks. Variations in the Sr/Ca ratio are due to changes in water infiltration to the cave prior and during the cave's warm season mode, where carbonate precipitation is most important. The extreme peaks in the Sr/Ca ratio can have two reasons:

I) a low amount of winter precipitation, or

II) warm winters are responsible for a reduced contribution of snow in precipitation and for early snow melting. The water from the early melting snow penetrates to the cave, when it is still in its cold season mode, where carbonate precipitation is small. Thus, less water infiltrates the cave during spring, when carbonate precipitation is more important.

The most likely reason for the Sr/Ca anomalies during the LIA is the low amount of winter precipitation. However, the western Tian Shan region appears to have experienced significant changes in climate during the recent past. An indication for this is that in the past 40 years the second mechanism seems to be responsible for high Sr/Ca ratios (and δ^{18}O). Thus, the response of climate proxies was shown to have been changed in time as seen in the course of modern climate warming. The evidence of this change in proxy interpretation at this location provides a strong reason to advice similar speleological studies to carefully assess present day relationships of climate parameters with respect to past climate conditions.

In this study, the covariation of δ^{18}O and δ^{13}C is used to deduce on the original δ^{18}O isotopic signature of infiltrating water entering the cave during the main stalagmite growth season. This new method in data reduction showed that the amount of winter precipitation in the western Tian Shan region varied strongly during the past millennium. It appears that the periods of strong decrease in winter precipitation occurred simultaneously to negative excursions of the winter NAO index. Also the low frequency behaviour of the stable O isotope composition is comparable with those of NAO reconstructions. Consequently, it is argued that the NAO index and the resulting strength and direction of winter Westerlies from the North Atlantic to Central Asia is the main driver for winter precipitation availability in the western Tian Shan region.

Acknowledgements

This research was supported by the Helmholtz Centre Potsdam (GFZ) Global Change Observatory of Central Asia (GCO-CA), and by the Central Asian Climate Dynamics Project (CADY), which was funded by Germany's Federal Ministry of Education and Research (BMBF). JF acknowledges funding by Deutsche Forschungsgemeinschaft (DFG) through grant FO809/4-1. We are grateful for B. Richert for µXRF scanning, and H. Meyer for water isotope analysis.

References

Aichner, B., Feakins, S. J., Lee, J. E., Herzschuh, U., Liu, X., 2015. High-resolution leaf wax carbon and hydrogen isotopic record of the late Holocene paleoclimate in arid Central Asia. Climate of the Past 11, 619-633.

Aizen, E. M., Aizen, V. B., Melack, J. M., Nakamura, T., Ohta, T., 2001. Precipitation and atmospheric circulation patterns at mid-latitudes of Asia. International Journal of Climatology 21, 535–556.

Aizen, V. B., Aizen, E. M., Melack, J. M., Dozier, J., 1997. Climatic and hydrologic changes in the Tian Shan, central Asia. Journal of Climate 10, 1393–1404.

Boch, R., Spötl, C., 2011. Reconstructing palaeoprecipitation from an active cave flowstone. Journal of Quaternary Science 26 (7), 675 – 687.

Bowling, D. R., McDowell, N. G., Bond, B. J., Law, B. E., Ehleringer, J. R., 2002. ^{13}C content of ecosystem respiration is linked to precipitation and vapour pressure deficit. Oecologia 131 (1), 113 – 124.

Bradley, R. S., Briffa, K. R., Cole, J., Hughes, M. K., Osborn, T. J., 2003. The climate of the last millennium. In: Paleoclimate, global change and the future. Springer, pp. 105–141.

Buchmann, N., Brooks, J. R., Rapp, K. D., Ehleringer, J. R., 1996. Carbon isotope composition of C4 grasses is influenced by light and water supply. Plant, Cell & Environment 19, 392–402.

Cerling, T. E., 1984. The stable isotopic composition of modern soil carbonate and its relationships to climate. Earth and Planetary Science Letters 71, 229 – 240.

Chen, F. H., Chen, J. H., Holmes, J., Boomer, I., Austin, P., Gates, J. B., Wang., N. L. Brooks, S. J., Zhang, J. W., 2010. Moisture changes over the last millennium in arid central Asia: a review, synthesis and comparison with monsoon region. Quaternary Science Reviews 29, 1055-1068.

Cruz Jr, F. W., Burns, S. J., Jercinovic, M., Karmann, I., Sharp, W. D., Vuille, M., 2007. Evidence of rainfall variations in southern Brazil from trace element ratios (Mg/Ca and Sr/Ca) in a rate Pleistocene stalagmite. Geochimica et Cosmochimica Acta 71 (9), 2250–2263.

Czernik, J., Goslar, T., 2001. Preparation of graphite targets in the Gliwice Radiocarbon Laboratory for AMS 14C dating. Radiocarbon 43, 283–292.

Deininger, M., Fohlmeister, J., Scholz, D., Mangini, A., 2012. The influence of evaporation effects on the carbon and oxygen isotope composition of speleothems - a model approach. Geochimica et Cosmochimica Acta 96, 57 – 79.

Dreybrodt, W., Scholz, D., 2011. Climatic dependence of stable carbon and oxygen isotope signals recorded in speleothems: From soil water to speleothem calcite. Geochimica et Cosmochimica Acta 75 (3), 734 – 752.

Dudashvili, S., and Dudashvilli, A., 2012. Caves in the region of Osh (russ.) ISBN978-9967-26-635-3, 188 pp.

Esper, J., Schweingruber, F. H., Winiger, M., 2002. 1300 years of climatic history for Western Central Asia inferred from tree-rings. The Holocene 12, 267–277.

Esper, J., Shiyatov, S. G., Mazepa, V. S., Wilson, R. J. S., Graybill, D. A., Funkhouser, G., 2003. Temperature-sensitive Tian Shan tree ring chronologies show multi-centennial growth trends. Climate Dynamics 21, 699–706.

Fairchild, I. J., Treble, P. C., 2009. Trace elements in speleothems as recorders of environmental change. Quaternary Science Reviews 28 (5-6), 449 – 468.

Favà, V., Curto, J. J., Llasat, M. C., 2016. Relationship between the summer NAO and maximum temperatures for the Iberian Peninsula. Theoretical and Applied Climatology 126, 77-91.

Feng, W., Casteel, R. C., Banner, J. L., Heinze-Fry, A., 2014. Oxygen isotope variations in rainfall, drip-water and speleothem calcite from a well-ventilated cave in Texas, USA: Assessing a new speleothem temperature proxy. Geochimica et Cosmochimica Acta 127, 233-250.

Fohlmeister, J., Kromer, B., Mangini, A., 2011a. The influence of soil organic matter age spectrum on the reconstruction of atmospheric ^{14}C levels via stalagmites. Radiocarbon 53 (1), 99 – 115.

Fohlmeister, J., Scholz, D., Kromer, B., Mangini, A., 2011b. Modelling carbon isotopes of carbonates in cave drip water. Geochimica et Cosmochimica Acta 75 (18), 5219 – 5228.

Fohlmeister, J., Schröder-Ritzrau, A., Scholz, D., Spötl, C., Riechelmann, D. F. C., Mudelsee, M., Wackerbarth, A., Gerdes, A., Riechelmann, S., Immenhauser, A., Richter, D. K., Mangini, A., 2012. Bunker Cave stalagmites: an archive for central European Holocene climate variability. Climate of the Past 8 (5), 1751–1764.

Fohlmeister, J., Schröder-Ritzrau, A., Spötl, C., Frisia, S., Miorandi, R., Kromer, B., Mangini, A., 2010. The influences of hydrology on the radiogenic and stable carbon isotope composition of cave drip water, Grotta di Ernesto (Italy). Radiocarbon 52 (4), 1529 – 1544.

Fohlmeister, J., Vollweiler, N., Spötl, C., Mangini, A., 2013. COMNISPA II: update of a mid-European isotope climate record, 11 ka to present. The Holocene 23, 747 – 752.

Folland, C. K., Knight, J., Linderholm, H. W., Fereday, D., Ineson, S., Hurrell, J. W., 2009. The summer North Atlantic Oscillation: past, present, and future. Journal of Climate 22, 1082–1103.

Frisia, S., Fairchild, I. J., Fohlmeister, J., Miorandi, R., Spötl, C., Borsato, A., 2011. Carbon mass-balance modelling and carbon isotope exchange processes in dynamic caves. Geochimica et Cosmochimica Acta 75, 380-400.

Genty, D., Baker, A., Massault, M., Proctor, C., Gilmour, M., Pons- Branchu, E., Hamelin, B., 2001. Dead carbon in stalagmite: Carbonate bedrock paleodissolution vs. ageing of soil organic matter. Implications for ^{13}C variations in speleothems. Geochimica et Cosmochimica Acta 65 (20), 3443 – 3457.

Genty, D., Labuhn, I., Hoffmann, G., Danis, P. A., Mestre, O., Bourges, F., Wainer, K., Massault, M., van Exter, S., Régnier, E., Orengo, P., Falourd, S., Minster, B., 2014. Rainfall and cave water isotopic relationships in two South-France sites. Geochimica et Cosmochimica Acta 131, 323-343.

Gong, D.-Y., Ho, C.-H., 2002. The Siberian High and climate change over middle to high latitude Asia. Theoretical and Applied Climatology 72, 1–9.

Gong, D.-Y., Wang, S.-W., Zhu, J.-H., 2001. East Asian winter monsoon and Arctic oscillation. Geophysical Research Letters 28, 2073–2076.

Goslar, T., Czernik, J., Goslar, E., 2004. Low-energy ^{14}C AMS in Poznan Radiocarbon Laboratory, Poland. Nuclear Instruments and Methods in Physics Research Section B: Beam Interactions with Materials and Atoms 223, 5–11.

Graham, N. E., Ammann, C. M., Fleitmann, D., Cobb, K. M., Luterbacher, J., 2011. Support for global climate reorganization during the Medieval Climate Anomaly. Climate Dynamics 37, 1217–1245.

Griffiths, M. L., Fohlmeister, J., Drysdale, R. N., Hua, Q., Johnson, K. R., Hellstrom, J. C., Gagan, M. K., Zhao, J.-x., 2012. Hydrological control on the dead-carbon content of a Holocene tropical speleothem. Quaternary Geochronology 14, 81 – 93.

Grove, J. M., 2004. Little ice ages: ancient and modern (2 volumes).

Hartman, G., Danin, A., 2010. Isotopic values of plants in relation to water availability in the Eastern Mediterranean region. Oecologia 162, 837–852.

Hendy, C. H., 1971. The isotopic geochemistry of speleothems – I. The calculation of the effects of different modes of formation on the isotopic composition of speleothems and their applicability as palaeoclimatic indicators. Geochimica et Cosmochimica Acta 35, 801 – 824.

Holzhauser, H., Magny, M., Zumbühl, H. J., 2005. Glacier and lake-level variations in West-Central Europe over the last 3500 years. The Holocene 15, 789 – 801.

Hua, Q., McDonald, J., Redwood, D., Drysdale, R., Lee, S., Fallon, S., Hellstrom, J., 2012. Robust chronological reconstruction for young speleothems using radiocarbon. Quaternary Geochronology 14, 67–80.

Huang, Y., Fairchild, I. J., 2001. Partitioning of Sr^{2+} and Mg^{2+} into calcite under karst-analogue experimental conditions. Geochimica et Cosmochimica Acta 65, 47–62.

Huang, Y. M., Fairchild, I. J., Borsato, A., Frisia, S., Cassidy, N. J., Mc-Dermott, F., Hawkesworth, C. J., 2001. Seasonal variations in Sr, Mg and P in modern speleothems (Grotta di Ernesto, Italy). Chemical Geology 175, 429 – 448.

Huang, X., Oberhänsli, H., Von Suchodoletz, H., Sorrel, P., 2011. Dust deposition in the Aral Sea: implications for changes in atmospheric circulation in central Asia during the past 2000 years. Quaternary Science Reviews, 30, 3661-3674.

Hurrell, J. W., 1995. Decadal trends in the North Atlantic oscillation: Regional temperatures and precipitation. Science 269, 676.

Hurrell, J. W., 1996. Influence of variations in extratropical wintertime teleconnections on Northern Hemisphere temperature. Geophysical Research Letters 23, 665–668.

Hurrell, J. W., Van Loon, H., 1997. Decadal variations in climate associated with the North Atlantic Oscillation. In: Climatic Change at High Elevation Sites. Springer, pp. 69–94.

Jones, P. D., Briffa, K. R., Osborn, T. J., Lough, J. M., Van Ommen, T. D., Vinther, B. M., Luterbacher, J., Wahl, E. R., Zwiers, F. W., Mann, M. E., et al., 2009. High-resolution palaeoclimatology of the last millennium: a review of current status and future prospects. The Holocene 19, 3–49.

Khalsa, S. J. S., Aizen, V. B., 2008. Variability in Central Asia seasonal snow cover during the MODIS period of record. In: Proceedings of 2008 IEEE International Geoscience & Remote Sensing Symposium. Vol. 10. pp. 1–2.

Lamb, P. J., Peppler, R. A., 1987. North Atlantic Oscillation: concept and an application. Bulletin of the American Meteorological Society 68, 1218–1225.

Lauterbach, S., Witt, R., Plessen, B., Dulski, P., Prasad, S., Mingram, J., Gleixner, G., Hettler-Riedel, S., Stebich, M., Schnetger, B., et al., 2014. Climatic imprint of the mid-latitude Westerlies in the central Tian Shan of Kyrgyzstan and teleconnections to North Atlantic climate variability during the last 6000 years. The Holocene 24, 970 – 984.

Lechleitner, F. A., Fohlmeister, J., McIntyre, C., Baldini, L., Jamieson, R. A., Hercman, H., Gasiorowski, M., Pawlak, J., Stefaniak, K., Socha, P., Eglinton, T. I., Baldini, J. U. L., 2016. A novel approach for construction of accurate radiocarbon-based chronologies for speleothems. Quaternary Geochronology 35, 54-66.

Linderholm, H. W., Seim, A., Ou, T., Jeong, J. H., Liu, Y., Wang, X., Bao, G., Folland, C., 2013. Exploring teleconnections between the summer NAO (SNAO) and climate in East Asia over the last four centuries–A tree-ring perspective. Dendrochronologia 31, 297-310.

Mayewski, P. A., Rohling, E. E., Stager, J. C., Karlén, W., Maasch, K. A., Meeker, L. D., Meyerson, E.A. Gasse, F., van Kreveld, S., Holmgren, K., Lee-Thorp, J., Rosqvist, G., Rack, F., Staubwasser, M., Schneider, R. R., Steig, E. J., 2004. Holocene climate variability. Quaternary Research 62, 243-255.

Meehl, G. A., Van Loon, H., 1979. The seesaw in winter temperatures between Greenland and Northern Europe. Part III: Teleconnections with lower latitudes. Monthly weather review 107, 1095–1106.

Meyer, H., Schoenicke, L., Wand, U., Hubberten, H. W., and Friedrichsen, H., 2000, Isotope studies of hydrogen and oxygen in ground ice-experiences with the equilibration technique: Isotopes Environ Health Stud, v. 36, no. 2, p. 133-149.

Mickler, P. J., Stern, L., Banner, J. L., 2006. Large kinetic isotope effects in modern speleothems. Geological Society of America Bulletin 118 (1/2), 65 – 81.

Morris, B. L., Darling, W. G., Gooddy, D. C., Litvak, R. G., Neumann, I., Nemaltseva, E. J., Poddubnaia, I., 2005. Assessing the extent of induced leakage to an urban aquifer using environmental tracers: an example from Bishkek, capital of Kyrgyzstan, Central Asia. Hydrogeology Journal 14, 225-243.

Mühlinghaus, C., Scholz, D., Mangini, A., 2009. Modelling fractionation of stable isotopes in stalagmites. Geochimica et Cosmochimica Acta 71, 2780 – 2790.

Niggemann, S., Mangini, A., Mudelsee, M., Richter, D. K., Wurth, G., 2003. Sub-Milankovitch climatic cycles in Holocene stalagmites from Sauerland, Germany. Earth and Planetary Science Letters 216, 539 – 547.

Olsen, J., Anderson, N. J., Knudsen, M. F., 2012. Variability of the North Atlantic Oscillation over the past 5,200 years. Nature Geoscience 5, 808 – 812.

Ortega, P., Lehner, F., Swingedouw, D., Masson-Delmotte, V., Raible, C. C., Casado, M., Yiou, P., 2015. A model-tested North Atlantic Oscillation reconstruction for the past millennium. Nature 523, 71-74.

Parker, L. W., Miller, J., Steinberger, Y., Whitford, W. G., 1983. Soil respiration in a Chihuahuan desert rangeland. Soil Biology and Biochemistry 15, 303-309.

Polag, D., 2009. Kinetic fractionation of stable isotopes in speleothems – laboratory and in situ experiments. Ph.D. thesis, Ruprecht-Karls-University Heidelberg.

Polag, D., Scholz, D., Mühlinghaus, C., Spötl, C., Schröder-Ritzrau, A., Segl, M., Mangini, A., 2010. Stable isotope fractionation in speleothems: Laboratory experiments. Chemical Geology 279, 31 – 39.

Reimer, P., Bard, E., Bayliss, A., Beck, J.W., Blackwell, P.G., Bronk Ramsey, C., Buck, C., Cheng, H., Edwards, R.L., Friedrich, M., Grootes, P.M., Guilderson, T.P., Haflidason, H., Hajdas, I., Hatte, C., Heaton, T.J., Hoffmann, D.L., Hogg, A.G., Hughen, K.A., Kaiser, K.F., Kromer, B., Manning, S.W., Niu, M., Reimer, R.W., Richards, D.A., Scott, E.M., Southon, J.R., Staff, R.A., Turney, C.S.M., van der Plicht, J., 2013. IntCal13 and Marine13 radiocarbon age calibration curves 0-50,000 years cal BP. Radiocarbon 55, 1869-1887

Riechelmann, D. F. C., Schröder-Ritzrau, A., Scholz, D., Fohlmeister, J., Spötl, C., Richter, D. K., Mangini, A., 2011. Monitoring Bunker Cave (NW Germany): A prerequisite to interpret geochemical proxy data of speleothems from this site. Journal of Hydrology 409, 682-695.

Rudzka, D., McDermott, F., Baldini, L. M., Fleitmann, D., Moreno, A., Stoll, H., 2011. The coupled δ13C-radiocarbon systematics of three late glacial/early Holocene speleothems; Insights into soil and cave processes at climatic transitions. Geochimica et Cosmochimica Acta 75 (15), 4321 – 4339.

Rudzka, D., McDermott, F., Surić, M., 2012. A late Holocene climate record in stalagmites from Modrič Cave (Croatia). Journal of Quaternary Science 27, 585-596.

Schimmelpfennig, I., Schaefer, J. M., Akcar, N., Koffman, T., Ivy-Ochs, S., Schwartz, R., Finkel, R. C., Zimmerman, S., Schlüchter, C., 2014. A chronology of Holocene and Little Ice Age glacier culminations of the Steingletscher, Central Alps, Switzerland, based on high-sensitivity beryllium-10 moraine dating. Earth and Planetary Science Letters 393, 220–230.

Schlesinger, W. H., 1977. Carbon balance in terrestrial detritus. Annual review of ecology and systematics 8, 51-81.

Schneider, U., Becker, A., Finger, P., Meyer-Christoffer, A., Rudolf, B., Ziese, M., 2011: GPCC Full Data Reanalysis Version 6.0 at 0.5°: Monthly Land-Surface Precipitation from Rain-Gauges built on GTS-based and Historic Data, DOI: 10.5676/DWD_GPCC/FD_M_V7_050

Scholz, D., Frisia, S., Borsato, A., Spötl, C., Fohlmeister, J., Mudelsee, M., Miorandi, R., Mangini, A., 2012. Holocene climate variability in North-Eastern Italy: Potential influence of the NAO and solar activity recorded by speleothem data. Climate of the Past 8, 1367 – 1383.

Seyd, F. S., Giorgi, F., Pal, J., Keay, K., 2010. Regional climate model simulation of winter climate over Central–Southwest Asia, with emphasis on NAO and ENSO effects. International Journal of Climatology 30, 220 – 235.

Sorg, A., Bolch, T., Stoffel, M., Solomina, O., Beniston, M., 2012. Climate change impacts on glaciers and runoff in Tian Shan (Central Asia). Nature Climate Change 2, 725 – 731.

Sorrel, P., Popescu, S.-M., Klotz, S., Suc, J.-P., Oberhänsli, H., 2007. Climate variability in the Aral Sea basin (Central Asia) during the late Holocene based on vegetation changes. Quaternary Research 67, 357 – 370.

Spötl, C., Fairchild, I. J., Tooth, A. F., 2005. Cave air control on dripwater geochemistry, Obir Caves (Austria): Implications for speleothem deposition in dynamically ventilated caves. Geochimica et Cosmochimica Acta 69, 2451-2468.

Spötl, C., Fohlmeister, J., Cheng, H., Boch, R., 2016. Modern aragonite formation at near-freezing conditions in an alpine cave, Carnic Alps, Austria. Chemical Geology 435, 60-70.

Stichler, W., Schotterer, U., Fröhlich, K., Ginot, P., Kull, C., Gäggeler, H., Pouyaud, B., 2001. Influence of sublimation on stable isotope records recovered from high-altitude glaciers in the tropical Andes. Journal of Geophysical Research: Atmospheres 106, 22613-22620.

Stoll, H. M., Müller, W., Prieto, M., 2012. I-STAL, a model for interpretation of Mg/Ca, Sr/Ca and Ba/Ca variations in speleothems and its forward and inverse application on seasonal to millennial scales. Geochemistry, Geophysics, Geosystems 13.

Stuiver, M., Polach, H. A., 1977. Discussion reporting of 14C data. Radiocarbon 19, 355 – 363.

Taft, L., Mischke, S., Wiechert, U., Leipe, C., Rajabov, I.,Riedel, F., 2014. Sclerochronological oxygen and carbon isotope ratios in Radix (Gastropoda) shells indicate changes of glacial meltwater flux and temperature since 4,200 cal yr BP at Lake Karakul, eastern Pamirs (Tajikistan). Journal of Paleolimnology, 52, 27-41.

Thompson, D. W. J., Wallace, J. M., Hegerl, G. C., 2000. Annular modes in the extratropical circulation. Part II: Trends. Journal of Climate 13, 1018 – 1036.

Treble, P., Shelley, J. M. G., Chappell, J., 2003. Comparison of high resolution sub-annual records of trace elements in a modern (1911 – 1992) speleothem with instrumental climate data from southwest Australia. Earth and Planetary Science Letters 216, 141 – 153.

Trouet, V., Esper, J., Graham, N. E., Baker, A., Scourse, J. D., Frank, D. C., 2009. Persistent positive North Atlantic Oscillation mode dominated the medieval climate anomaly. Science 324, 78 – 80.

Trouet, V., Scourse, J. D., Raible, C. C., 2012. North Atlantic storminess and Atlantic Meridional Overturning Circulation during the last Millennium: Reconciling contradictory proxy records of NAO variability. Global and Planetary Change 84, 48 – 55.

van Loon, H., Rogers, J. C., 1978. The seesaw in winter temperatures between Greenland and northern Europe. Part I: General description. Monthly Weather Review 106, 296 – 310.

Vuille, M., Bradley, R. S., Healy, R., Werner, M., Hardy, D. R., Thompson, L. G., Keimig, F., 2003. Modeling $\delta^{18}O$ in precipitation over the tropical Americas: 2. Simulation of the stable isotope signal in Andean ice cores. Journal of Geophysical Research: Atmospheres 108, 4175.

Wackerbarth, A., Scholz, D., Fohlmeister, J., Mangini, A., 2010. Modelling the δ18O value of cave drip water and speleothem calcite. Earth and Planetary Science Letters 299, 387 – 397.

Wanner, H., Brönnimann, S., Casty, C., Gyalistras, D., Luterbacher, J., Schmutz, C., Stephenson, D. B., Xoplaki, E., 2001. North Atlantic Oscillation – concepts and studies. Surveys in Geophysics 22, 321 – 381.

Wassenburg, J., Dietrich, S., Fietzke, J., Fohlmeister, J., Jochum, K. P., Scholz, D., K., R. D., Sabaoui, A., Sptl, C., Lohmann, G., Wei, W., Andreae, M., Immenhauser, A., 2016. Major reorganization of the North Atlantic Oscillation during Early Holocene deglaciation. Nature Geoscience 9, 602-605.

Wiedner, E., Scholz, D., Mangini, A., Polag, D., Mühlinghaus, C., Segl, M., 2008. Investigation of the stable isotope fractionation in speleothems with laboratory experiments. Quaternary International 187, 15–24.

Willmott, C. J., Matsuura, K., 2001. Terrestrial air temperature and precipitation: Monthly and annual time series (1950 - 1999), http://climate.geog.udel.edu/~climate/html_pages/README.ghcn_ts2.html.

Wolff, Ch., Plessen, B., Dudashvili, A., Breitenbach, S.F.M., Cheng, H., Edwards, L.R., Strecker, M.R., 2017, Precipitation evolution of Central Asia during the last 5000 years. The Holocene 27, 142-154.

Supplementary material for:

Winter precipitation changes during the Medieval Climate anomaly and the Little Ice Age in Central Asia

Jens Fohlmeister [1,*], Birgit Plessen [2], Alexey Sergeevich Dudashvili [3], Rik Tjallingii [2], Christian Wolff [1,4], Abror Gafurov [5] , Hai Cheng [6,7]

1 Institute of Earth and Environmental Science, University of Potsdam, Karl-Liebknecht-Strasse 24, D-14476, Germany

2 Helmholtz Centre Potsdam, GFZ German Research Centre for Geosciences, Section 5.2 Climate Dynamics and Landscape Development, Telegrafenberg, D-14473 Potsdam, Germany

3 Fund of Preservation and Exploration of Caves (Kyrgyzstan)

4 Max Planck Institute for Chemistry, Climate Geochemistry Department, D-55128 Mainz, Germany

5 Helmholtz Centre Potsdam, GFZ German Research Centre for Geosciences, Section 5. 4 Hydrology, Telegrafenberg, D-14473 Potsdam, Germany

6 Institute of Global Environmental Change, Xi'an Jiaotong University, Xi'an, Shaanxi, 710049, China

7 Department of Geology and Geophysics, University of Minnesota, Minneapolis, MN 55455, USA

* corresponding author; contact details:
email: jens.fohlmeister@geo.uni-potsdam.de,
Tel: 0049 (0)331 9775435

Supplemental text:

A1

Conversion of d18O in precipitation (VSMOW) to d18O in carbonates (VPDB)

The mean d18O in the stalagmite carbonate is approximately -10.5‰ VPDB, when neglecting the positive d18O anomalies. In case this carbonate precipitated from water in equilibrium the approximate drip water d18O value on the VPDB scale is -40.9‰. For this calculation we used a temperature of 15°C (mean warm season cave temperature) and the fractionation factors of Kim and O Neil. (1997). Transferring the d18O value of drip water from the VPDB scale to VSMOW results in approximately -11.2‰ VSMOW. Such low values show that winter contribution must be an important endmember for the drip water and carbonate.

A2

Isotope track along the outer part of the stalagmite

In addition to the central isotope track, a second isotope track along the flank of the stalagmite was measured. In the top part of the stalagmite the growth layers are significantly thinner on the second isotope track than on the centre isotope track (see Fig. 2). In the bottom part of the stalagmite no strong thinning in the growth layers at track two is observed. Despite this difficulty, both isotope systems show the same signal, although in the isotope track along the flank of the stalagmite, not all positive anomalies are present due to the growth layer thinning and lower sampling resolution (supplementary Fig. 3).

A3

Snow cover characteristics on the Keklik-Too mountain

For the analysis of the snow cover characteristics on the Keklik-Too mountain we used the Moderate Resolution Imaging Spectroradiometer (MODIS) snow cover product (Hall et al, 2006). The MODIS snow cover data is globally available since March 2000 and has a spatial resolution of 500 meters. The MODSNOW-Tool (Gafurov, et al, 2016) was used to process raw MODIS snow cover data including cloud elimination for the entire Aravansay River basin (supplementary Fig. 4).

Supplementary Fig. 4a shows that Keklik-Too mountain is located close to the outlet of Aravansay River Basin. Snow cover duration in mountainous regions with higher altitudes (southern part) is longer. The snow cover duration on Bir-Uja Cave varies year to year and was on average 67 days in the last 17 years (supplementary Fig. 4b). Temporal variation of snow cover fraction of the Keklik-Too shows that during the last 17 years the snow often melted away within the middle of winter (End of December and January, supplementary Fig. 4c). This was too early to contribute melt water to the stalagmite growth season, which is starting in May. The main snow melt event started latest in the end of February. This water could contribute to the cave drip water, when accounting a few months of water residence time in the karst.

Supplemental figures:

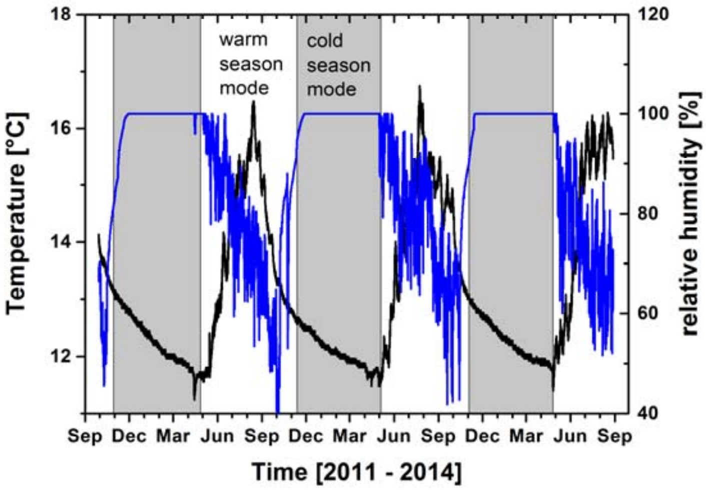

Fig. 1: Logged cave temperature (black) and relative humidity (blue) in short distance to the location of stalagmite Keklik1. Cave ventilation is responsible for two modes: I) cold season mode: relative humidity is 100% and temperature is decreasing to the mean annual atmospheric temperature and II) warm season mode: relative humidity is decreasing to about 60% and cave temperature increases, peaks at about 16°C in August and start to decrease afterwards. According to the logged relative humidity, the cold season mode (grey background) is between end of November and April and the warm season mode is between May to October.

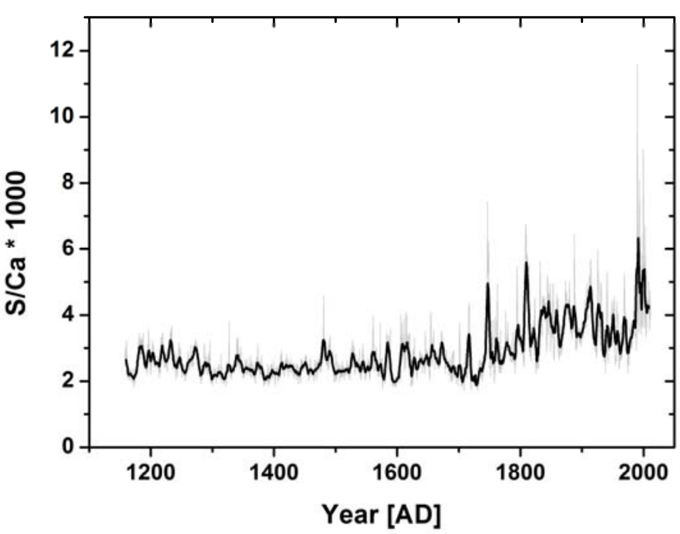

Fig. 2: Sulphur content of Keklik 1. A remarkable increase in the S/Ca ratio is observed between1750 and 1850 AD. This is related to the rise of industry during the industrial revolution starting in the midth of the 18th century. Thus the S/Ca ratio supports the age-depth relationship established by the new radiocarbon method (Lechleitner et al., 2016).

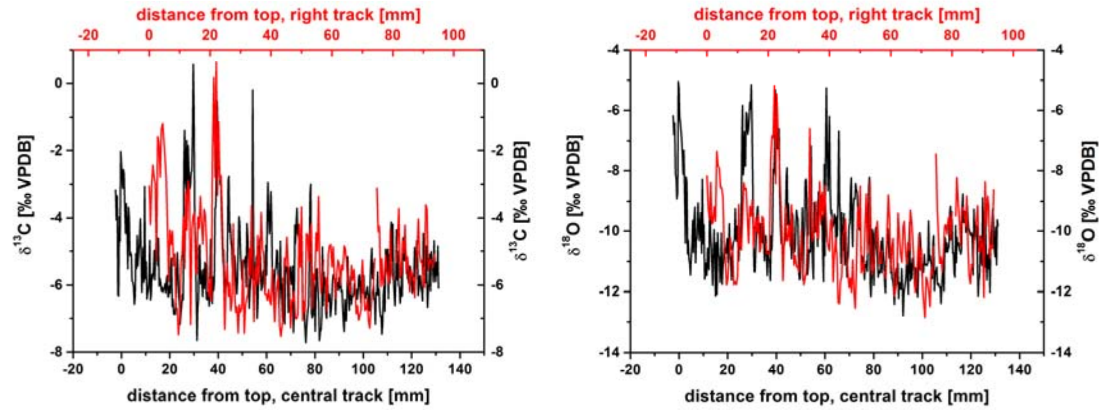

Fig. 3: Stable C isotope composition (left) and the stable O isotope composition (right) of the central track (black) and outer track on the right flank of Keklik1 (red). Both depth scales are adjusted to fit the main isotope anomalies. However, due to the significant thinning of the growth layers in the upper part of Keklik1 (apparently slower growth in the right track than along the central track) the top section of the right track does not fit perfectly. No attempts were made to manually stretch the outer track to better fit the central track. The level of the isotope values for the track along the flank has generally higher $\delta^{13}C$ and $\delta^{18}O$ values than the track along the growth axis. This is due to fractionation processes along the flank of the stalagmite during stalagmite growth. The significant thinning of growth layers at the flank is also responsible to not detect all positive isotope anomalies to their full range. The increase of the C and C isotopic composition at the very top is not recorded in track along the flank of the stalagmite.

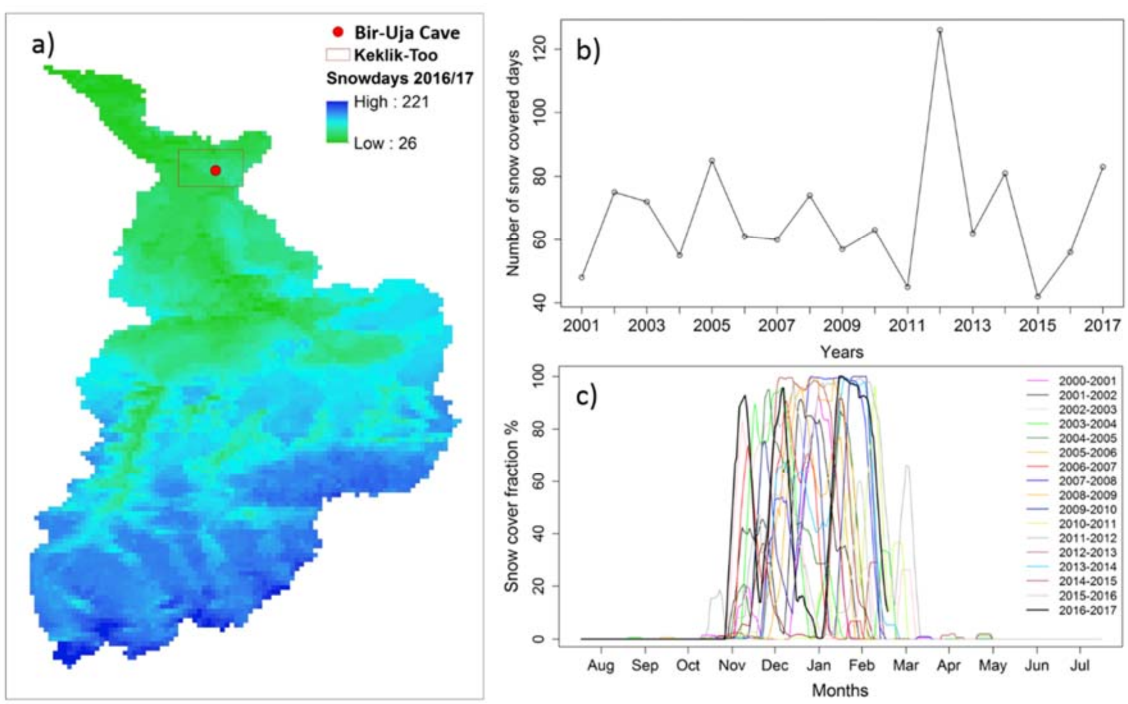

Fig. 4: Snow cover characteristics of the Keklik-Too mountain. a) Number of snow days for each pixel in the catchment area of the Aravansay for the hydrological year 2016/2017. The Keklik-Too

mountain is within the red rectangle and the cave location is marked by the red circle. b) Number of snow days of the pixel covering Bir-Uja Cave from 2001 to 2017. c) Temporal variation of snow cover fraction relative to the area covering Keklik-Too mountain (red rectangle).

Supplemental tables:

Tab. 1: Water oxygen isotopic composition and element distribution. All element concentrations are given in ppb.

Date	T_{water}	$\delta^{18}O$ [‰ vs SMOW]	δD [‰ vs SMOW]	Si	Al	K	Ca	Sr	Mg	U	Cu
05.10.11	15° C	-6.6	-56.3	33559	709	4677	244630	1726	66728	3.7	131
21.05.12	13° C	-12.8	-91.4	27575	498	4599	25661	141	4543	0.8	2
04.09.14	16° C	-6.2	-62.1	45624	29549	4496	278569	674	20685	2.0	7

Tab. 2: Slope between $\delta^{13}C$ (X) and $\delta^{18}O$ (Y) along the pathway of carbonate precipitation. Cave experiments as well as cave analogue laboratory experiments are listed.

Slope	Cave/laboratory	study
0.27	Bunker cave	Polag, 2009
0.27	B7 cave	Polag, 2009
0.48	B7 cave	Polag, 2009
0.25	Harrison's Cave	Mickler et al., 2006
0.43-0.75	laboratory (various parameters)	Polag 2009; Polag et al., 2010
0.71	laboratory	Wiedner et al., 2008

References

Gafurov, A., Lüdtke, S., Unger-Shayesteh, K., Vorogushyn, S., Schöne, T., Schmidt, S., Kalashnikova, O., Merz, B., 2016. MODSNOW-Tool: an operational tool for daily snow cover monitoring using MODIS data. Environmental Earth Sciences 75, 1-15.

Hall, D. K., Salomonson, V. V., Riggs. G. A., 2006. *MODIS/Terra Snow Cover Daily L3 Global 500m Grid, Version 5*. [Indicate subset used]. Boulder, Colorado USA. NASA National Snow and Ice Data Center Distributed Active Archive Center. doi: http://dx.doi.org/10.5067/63NQASRDPDB0.

Kim, S. T., O'Neil, J. R., 1997. Equilibrium and non-equilibrium oxygen isotope effects in synthetic carbonates. Geochimica et Cosmochimica Acta 61, 3461-3475.

Lechleitner, F. A., Fohlmeister, J., McIntyre, C., Baldini, L., Jamieson, R. A., Hercman, H., Gasiorowski, M., Pawlak, J., Stefaniak, K., Socha, P., Eglinton, T. I., Baldini, J. U. L., 2016. A novel approach for construction of accurate radiocarbon-based chronologies for speleothems. Quaternary Geochronology 35, 54-66.

Mickler, P. J., Stern, L., Banner, J. L., 2006. Large kinetic isotope effects in modern speleothems. Geological Society of America Bulletin 118 (1/2), 65 – 81.

Polag, D., 2009. Kinetic fractionation of stable isotopes in speleothems – laboratory and in situ experiments. Ph.D. thesis, Ruprecht-Karls-University Heidelberg.

Polag, D., Scholz, D., Mühlinghaus, C., Spötl, C., Schröder-Ritzrau, A., Segl, M., Mangini, A., 2010. Stable isotope fractionation in speleothems: Laboratory experiments. Chemical Geology 279, 31 – 39.

Wiedner, E., Scholz, D., Mangini, A., Polag, D., Mühlinghaus, C., Segl, M., 2008. Investigation of the stable isotope fractionation in speleothems with laboratory experiments. Quaternary International 187, 15–24.